Supplementary Discussion

Population naming

In some contexts, the indigenous hunter-gatherer and pastoralist peoples of southern Africa are referred to collectively as the Khoisan (Khoi-San) or more recently Khoesan (Khoe-San) people. This grouping is based on the unique linguistic use of click-consonants[1]. Many names, often country-specific, have been used by Bantu pastoralists and European settlers to describe the hunter-gatherers, including San, Saan, Sonqua, Soaqua, Souqua, Sanqua, Kwankhala, Basarwa, Batwa, Abathwa, Baroa, Bushmen, Bossiesmans, Bosjemans, or Bosquimanos. In addition, group-specific names such as !Kung and Khwe are often used for the broader population. The two most commonly used names, "San" and "Bushmen", have both been associated with much controversy due to derogatory connotations[2]. "San" has become the more popular term used in Western literature, although "Bushmen" is arguably the more commonly recognized term within the communities. Since they have no collective name for themselves, the term Bushmen was selected for use in this paper as the term most familiar to the participants themselves.

Regarding identification of individuals

The five men identified in this study have all elected to have their identity made public knowledge. Thus we present two complete personal genomes (KB1 and ABT), a low-coverage personal genome (NB1), and personal exomes for all five men. On a scientific level, identification allows for current and future correlation of genetic data with demographic and medical histories. On a social level, identification allows for maximizing community benefit. For !Gubi, G/aq'o, D#kgao and !Aî, their name represents not only themselves, but importantly their extended family unit and a way of life severely under threat. For Archbishop Desmond Tutu, his international status will have an immediate impact on providing a voice for southern Africa in pharmaceutical developments based on genomic data.

Ethics approval

Ethics approval to conduct whole-genome sequencing and/or extended genetic diversity studies was obtained from the Institutional Review Board (IRB) or Human Research Ethics Committee (HREC) from three institutions, namely the Pennsylvania State University (IRB #28460 and IRB #28890), the University of New South Wales, Australia (HREC #08089 and HREC #08244), and the University of Limpopo, South Africa (Limpopo Provincial Government #011/2008). All authors directly involved with the study participants and/or data generated are named on one or more approvals. A study permit was obtained from the Ministry of Health and Social Services (MoHSS), Namibia. In addition to the named institutions, an external advisory panel of South African academic and medical professionals was established on the recommendation of Archbishop Tutu. Informed consent was obtained either via written or video-recorded (in cases of illiteracy) documentation. For the Bushmen, consent was performed in three languages and in the presence of a caretaker and translator. All participants undergoing genome sequencing elected to be named in the study. Study participants underwent extensive face-to-face interviews and have been fully advised about the outcomes of the research. During the site visits, there was no change in the desire to participate in this study. All participants provided venous whole blood, and DNA was extracted using standard extraction procedures (Qiagen Inc., Hilden, Germany).

Participant selection

The southern African Bushmen have been proposed to show increased within-group Y-chromosome diversity and limited overall mtDNA diversity[3]. Therefore, we examined males exclusively, to increase the amount of detectable variation. Each of the four participating indigenous hunter-gatherer individuals is the eldest member of his community. Additional criteria for inclusion in the study were based on linguistic group, geographical location, and the presence of previously described population-specific non-recombining Y-chromosome (NRY) markers[4] (Figure 1, Supplementary Table 1).

A total of 20 Bushmen were genotyped via amplicon-specific Sanger sequencing for 13 Y chromosome markers[5] (M2, M9, M14, M35, M51, M90, M98, M112, M115, M150, M154, M175, and M211). The group consisted of 19 Juu-speakers (13 Ju/'hoansi, four Etosha !Kung, two Vasekela !Kung), and a single Tuu-speaker. "Vasekala" is a local term for a group relocated from Angola to the northern Kalahari region of Namibia after serving in the South African Defense Force during the Namibian-Angolan war. Several candidates were excluded because of their non-African (K-R) and Asian/Indonesian haplogroups (O); two were excluded because of a Bantu-dominant E1b1a (previously known as E3a) haplotype.

The indigenous Kalahari Juu- and Tuu-speaking hunter-gatherers included in this study live in scattered family groups in the vast semi-desert regions of Namibia, an 823,145-km^2 country on the southwest coast of Africa with approximately 2 million inhabitants. Namibia is home to around 38,000 Bushmen[6]. KB1, !Gubi, is the only member of the study belonging to the poorly defined Tuu-speaking group of the southern Kalahari. NB1, G/aq'o, and TK1, D#kgao, are both Ju/'hoansi of the northern Kalahari region, separated by approximately 120 km. MD8, !Aî, belongs to the !Kung-speaking group relocated some 50 years ago from the Etosha plains region in the northwestern Kalahari. The Ju/'hoansi and !Kung are grouped linguistically as Juu-speakers. The four Bushmen participants represent Y haplogroups A2 (TK1), A3b1 (NB1), B2b (KB1), and E1b1b1 (MD8).

Archbishop Desmond Tutu (ABT) is directly descended from the two major linguistic groups in southern Africa, namely the Nguni-speakers (approximately 60% of the people of South Africa) via his paternal Xhosa ancestry and from the Sotho-Tswana-speakers (approximately 33% of the people of South Africa) via his maternal Motswana ancestry. These two linguistic groups therefore represent over 90% of the South African Bantu population, who have lived along-side the indigenous hunter-gatherer and herder peoples (Khoesan) for over 2,000 years. Archbishop Tutu is thus an ideal representative of the southern African Bantu peoples. Using genome-wide genotypes and whole-genome sequence data, ABT was classified in the E1b1a8a Y-haplogroup.

Genome-wide heterozygosity and potential admixture

Evaluation of population admixture within our study's four Bushmen required a genotypic analysis of a southern African Bantu population. For this study, we elected to use data previously generated for the Xhosa (XHO), the paternal lineage of Archbishop Tutu. Linguistically, the Xhosa have adopted "click" consonants within their language, suggesting an extensive period of cohabitation with the indigenous hunter-gatherers.

Since one indicator of admixture is an elevated rate of heterozygosity, we used genome-wide genotyping data (from Illumina 1M Human Duo arrays) to determine the overall percentage

of heterozygosity in our five participants, plus a South African European (SAE) and an admixed South African Coloured (SAC) (Supplementary Figure 3A). The SAC community arose as a consequence of slavery and a subsequent genetic mixing of East African, East Indian, and Indonesian elements, starting with European settlement at the Cape in 1652. In a previous study we identified a European (predominantly via paternal lines) and southern African Bantu or East Asian (via maternal lines) admixture in this community, with negligible Bushmen contribution[7].

Increased overall percentage heterozygosity in MD8 compared to KB1, NB1, and TK1 may indicate a degree of admixture. However, we were surprised that the heterozygosity determined by this method was on average low in the Bushmen, particularly since our sequence data indicate otherwise. The observed low heterozygosity suggests one (or more likely a combination of) the following scenarios: (1) population isolation, (2) reduced admixture events, and (3) reduced informativeness of this particular SNP array for Bushmen. The observed low percentage heterozygosity in ABT compared to SAE and SAC populations also may be an artifact of using a European-biased array.

Autosome-specific analysis of heterozygosity (Supplementary Figure 3B) demonstrated sample-specific hotspots, for example the increased percentage heterozygosity observed in chromosome 5 for KB1 and the reduced heterozygosity observed in chromosome 18 for TK1, compared to the other Bushmen.

Impact of traditional life-style on gender-biased gene flow

The reported limited male-mediated gene flow[8] in southern African Bantu populations[9] has resulted in a predominance of the E1b1a (M2) Y-chromosome haplogroup across the region. Lack of Y-chromosome divergence has been attributed to cultural practices of patrilocality (location of family with that of the male) and polygyny (multiple wives), resulting in a lower male migration rate and lower male effective size, respectively[10]. In contrast to their Bantu neighbors, the indigenous hunter-gatherers practice a culture of matrilocality and monogyny; thus we can assume a male-biased migration rate resulting in greater Y-chromosome over mtDNA diversity.

Traditionally, due to a nomadic lifestyle, the hunter-gatherer people do not own possessions. This lack of ownership results in Bushmen men being ineligible to marry a Bantu woman, because they cannot pay the father-in-law a “lobola” (also known as lobolo or mahadi), a payment usually made in cattle for her hand in marriage. Male-contributed Bushmen-Bantu admixture is therefore assumed to be minimal to absent. Bantu men marrying hunter-gatherer women is however reported to have been quite common. A feeling of inferiority associated with the “Bushmen” or “San” ethnic classification meant that many Bushmen women tried to uplift their status via marriage to Bantu men. We therefore speculate the strong possibility of Bushmen contributions to the mitochondrial genome and X-chromosome in southern African Bantu populations.

Insertions, deletions, microsatellites, and Alu elements

We identified 463,788 putative short indels (i.e., insertions/deletions; the longest was 38 bp) in the KB1 genome, of which 172,589 (37.2%) are homozygous. A special class consists of small indels created by expansion or contraction of a microsatellite, here taken to mean a tandem duplication of a core sequence of between 2 and 6 nucleotides. We identified 102,476 high-confidence microsatellites, each having no differences among its tandem copies and separated by sharp boundaries from the flanking non-repetitive DNA. For 16.0% of these, the number of

copies of the core sequence appeared to differ from the orthologous repeats in the hg19 (a human reference genome that superseded the one used for most of our analyses), Venter, and/or Watson genomes. We also inspected KB1's exome to determine his genotype at unstable microsatellites in which mutations (usually expansions) have been documented or suggested to lead to disease[11]. At several such loci (Supplementary Table 15), alleles in KB1 possessed a number of repeats that was close to the minimum value in the normal range, suggesting that longer, disease-causing alleles were likely acquired by the non-Bushmen lineage later in its evolution.

The length distribution of longer indels (say, at least 50 bp relative to the human reference) in KB1 shows the expected enrichment at a length of around 300 bp caused by Alu interspersed-repeat elements, which are known to be polymorphic in the human population. We identified 503 Alu insertions in the human reference relative to the KB1 genome, with 44.1% belonging to the AluYa5 subfamily. Of these 503, we found 24 common to Watson, Venter, and the human reference, but absent in chimp, KB1 and NB1. Those Alu elements may have been inserted into the ancestor of non-Bushmen genomes after their divergence from the Bushmen lineage.

A portion (9.7%) of our Roche/454, non-paired reads do not map to the human reference genome at the thresholds we used (97% identity over at least 90% of the read). It has been reported[12,13] that the Roche instrument is capable of sequencing regions that are recalcitrant to the BAC-based approach used to sequence the reference. Indeed, a number of the unmapped reads align to regions of the chimpanzee genome that appear to be orthologous to human regions corresponding to gaps in the current human reference assembly. For instance a 200-kb gap in NCBI Build 36 at chromosome 6q16.1 corresponds to a chimpanzee interval where our unmapped reads produce 7.1X average read depth and assemble into 129 contigs of total length 253,769 bp. In other cases, we find assemblies of KB1 reads that contain exons apparently deleted from the reference assembly, e.g., parts of the GenBank mRNA sequences AK096045 and AK128592.

Genotype and phenotype correlations: lactase persistence

Lactase persistence (the ability to digest milk as adults) is an autosomal-dominant trait that is common in European-derived populations. This evolutionary adaptation has been associated with a SNP in intron 13 of the *MCM6* gene on chromosome 2, upstream of the gene encoding for lactase (*LCT*). This regulatory SNP, known as -13910 C>T (rs4988235), has been shown to increase *LCT* transcription in vitro by generating an Oct-1 transcription-factor binding site (reviewed in ref. 14). However, in contrast to Europe, the frequency of this allele in sub-Saharan Africa is rare, and it has not been found in the remains of Neolithic Europeans. These studies suggest that lactase persistence is an evolutionary innovation that has undergone strong population-specific positive selection following human conversion (via either a population replacement or cultural exchange) from forager to farmer. As expected for a foraging society, we found the Bushmen in our study all to be homozygous for the C-allele, suggesting an inability to tolerate milk consumption as adults.

Human pigmentation

A functional SNP that has undergone genetic selection in Europeans resulting in near fixation is the non-synonymous rs1426654 G>A (Ala111Thr) variant in the human pigmentation gene *SLC24A5*. The A-allele has undergone positive selection in the last 100,000 years, contributing to the pale skin color of Europeans. The color of the human skin is largely determined by the

amount and type of melanin pigment produced in the cutaneous melanocytes, which in turn impacts susceptibility to skin cancer, a condition mostly affecting people of pale complexion. The *SLC24A5* genotype observed in the sequence data was validated using TaqMan allelic discrimination for our sequenced men and additional individuals, demonstrating a predominance of the melanin-producing G-allele in the lighter-skinned Bushmen (allele frequency 0.98, n=45), and darker-skinned southern African Bantus from the same region (allele frequency 0.90, n=31), while being uncommon in pale-skinned southern African Europeans (allele frequency 0.07, n=14). Retaining this allele would provide a selective advantage for survival in the harsh climate of the Kalahari Desert.

Human pigmentation, however, is a polygenic quantitative trait with high variability influenced by a number of candidate genes. A recent genome-wide association study (GWAS) of natural hair color (a marker for pigmentation) identified two key polymorphisms, one located in another potassium-dependent sodium/calcium exchanger gene *SLC2A4A* (rs12896399 G>T)[15]. Significantly associated with light hair color, we found this allele to be absent in our sequenced men. These observations highlight the need for synergy between environment and phenotypic attributes, allowing for reproductive advantage and survival.

Duffy null allele

The Duffy antigen/receptor for chemokines (*DARC*) gene on chromosome 1 harbors a functional polymorphism in the promoter region (T-46C; rs2814778) responsible for the observed decreased white blood cell count in African-Americans compared with European-Americans[16,17]. The consequence is critical for medical conditions where decreased white cell levels are associated with diseases involving inflammation and infection. This so-called Duffy Null polymorphism (also known as *FY+/-*) has been associated with an evolutionary advantage in African populations due to protection against *Plasmodium vivax* malaria infection[18]. More recently, an association with susceptibility to HIV-1 infection has been reported[19]. This functional variant therefore has critical health implications relevant to southern African populations. The C-allele in Africans and T-allele in Europeans have reached almost complete population fixation. It has been suggested that the C-allele may have arisen in Africa as a result of selective pressure from a more lethal ancestral form of *Plasmodium vivax*[20]. The Asian origin hypothesis of *Plasmodium vivax* may suggest that fixation in Africa took place after the introduction of agriculture[21]. The lack of the C-allele in our forager participants (unlike the Bantu farmers) supports this latter hypothesis. We can further speculate that lack of agricultural adaptation in this community may be responsible for the absence of this allele and question what impact forced adaptation from forager to farmer will have on this already dwindling population.

CYP2G

KB1 and NB1 are homozygous for a SNP that retains the function of the *CYP2G* gene (Supplementary Table 6). While this gene encodes a cytochrome P450 monooxygenase involved in steroid metabolism in the olfactory mucosa of mice, it is not active in most humans because of a nucleotide substitution leading to premature termination of translation[22]. The Bushmen genomes encode an amino acid at this position rather than a stop codon, and thus are likely to produce an active enzyme (Supplementary Figure 8A). Indeed, their sequence is the same as the ancestral sequence at this position. This suggests that Bushmen retain the active gene, perhaps in response to selective pressure, but in other populations it has decreased in frequency (20% of Bantu[22]) or been lost (almost all non-African humans have inactive genes), presumably from

relaxation of selection.

Further analysis of this variant by Sanger sequencing confirmed genotype calls for KB1 and NB1, and identified homozygosity for this allele in 27% of our extended Bushmen group (8/30) and 7% of Bantus from the same region (2/29). All remaining samples, including 11 Europeans, were heterozygous for the active ancestral and inactive modern alleles. Distribution of alleles occurred in a 2:1 ratio in all cases (Supplementary Figure 8B). A likely explanation is that *CYP2G* is an unprocessed pseudogene formed by segmental duplication, which resulted in one copy becoming silenced by a degenerative mutation (the T-allele). The T-allele was the most common allele in all samples of European origin. Sequencing was confirmed in both directions.

CYP2E1

CYP2E1 is the major ethanol-inducible cytochrome P450 enzyme that metabolizes and activates many toxicologically important compounds, including ethanol, to more reactive toxic products. In fact, induction of *CYP2E1* is one of the central pathways by which ethanol generates oxidative stress via the generation of reactive oxygen species (ROS) such as superoxide anion radicals and hydrogen peroxide, and in particular of powerful oxidants like 1-hydroxyethyl radicals in the presence of iron catalysts. Ethanol-induced oxidative stress plays a major role in the mechanisms by which ethanol produces liver injury. We have detected and validated a 140-kb duplication encompassing the *CYP2E1* gene in KB1 (Supplementary Figure 6A) and previously described[23].

Variants in genes for lipid metabolism

We were intrigued by the apparent over-abundance of differences from the human reference genome in genes related to lipid metabolism (Supplementary Table 6). The diet of the non-pastoralist Bushmen is low in fats, and thus they may possess genetic variants associated with aspects of lipid metabolism not observed in other, pastoralist populations. We found that KB1, NB1, and ABT are heterozygous for a variant in the *LIPA* gene, which encodes lysosomal acid lipase, an enzyme that catalyzes hydrolysis of cholesterol esters and triglycerides. Mutations in *LIPA* that drastically reduce enzymatic activity lead to accumulation of cholesterol esters and triglycerides in the visceral organs, manifesting as a range of disorders including Wolman disease, a severe condition with onset in infants, and the milder cholesterol ester storage disease[24]. The G to A transition (C to T in chromosomal order; Supplementary Table 6) in the first position of codon 23 of *LIPA* causes a replacement of glycine by arginine in the signal peptide (Supplementary Figure 7). This transition was previously observed in a homozygous compound mutation in a Wolman disease proband[25]. While one of the sequence changes abolished enzymatic activity, the glycine to arginine replacement in the signal peptide had no effect on lipase activity. Instead, it substantially reduced the amount of enzyme secreted from cells. The fact that this allele is present in a heterozygous state in KB1, NB1, and ABT suggests that it is common in this population; previous studies estimated its frequency in healthy control individuals at only 0.05[26]. Thus while one may expect the arginine form of the enzyme to have reduced secretion, it may not be a problem and in fact could even provide some advantage, as many other mammals have an A at this position (Supplementary Figure 7).

A further complication to the interpretation of this variant is that an A to C polymorphism is found in codon 16, still in the signal peptide (Supplementary Figure 7). This second SNP, which is found in TK1 (homozygous), NB1, and ABT, changes the threonine encoded in the reference sequence (ACC) to a proline (CCC). If the threonine to proline SNP is also present in

the allele with the glycine to arginine SNP, then the second amino acid change could affect the secretion properties of the enzyme.

We tested the hypothesis that the sequenced Bushmen genomes have a higher SNP rate that other ethnic groups in genes related to lipid metabolism. We focused on the following genes: *AACS*, *ABCA1*, *ABCD1*, *ABHD5*, *ACADL*, *ACADM*, *ACADS*, *ACADVL*, *ACAT1*, *ACSL1*, *ALDH3A2*, *ANGPTL4*, *APOA2*, *ARSA*, *ASAH1*, *ASIP*, *CLN3*, *CLPS*, *CPT1A*, *CPT1B*, *CPT1C*, *CPT2*, *CYP27A1*, *DECR1*, *DHCR7*, *EHHADH*, *ETFDH*, *FADS2*, *GALC*, *GBA*, *GLA*, *GLB1*, *GM2A*, *HADH*, *HADHA*, *HADHB*, *HEXA*, *HEXB*, *HMGCL*, *HMGCS1*, *LIPA*, *LIPE*, *LIPF*, *LPIN2*, *LPL*, *MLYCD*, *MTTP*, *NPC1*, *NPC2*, *PLA2G1B*, *PLTP*, *PNLIP*, *PNPLA2*, *PSAP*, *SAR1B*, *SCP2*, *SLC22A5*, *SLC25A20* and *SMPD1*. Pooling the Bushmen's amino-acid SNPs, we found that 90 of their 23,430 SNPs were in these lipid-related genes. For a pooled sample of six non-Bushmen, 126 of 36,296 SNPs were in these genes. The ratio for Bushmen (0.384%) was slightly higher than for non-Bushmen (0.347%), but the following reasoning shows that the difference is not significant.

We have n=23,430 approximately independent trials with x=90 successes from a population with success probability p, and m=36,296 aproximately independent trials with y=126 successes from a population with success probability q. We want to test the null hypothesis $p=q$ against the alternative $p>q$. Because of the very large number of trials, under the null hyothesis, the test statistic:

$$Z = \frac{\frac{x}{n} - \frac{y}{m}}{\sqrt{\left(\frac{x+y}{n+m}\right)\left(1 - \frac{x+y}{n+m}\right)\left(\frac{1}{n} + \frac{1}{m}\right)}}$$

has approximately an N(0,1) normal distribution. The observed value of the statistic is:

$$Z = \frac{0.00384 - 0.00347}{\sqrt{\left(\frac{216}{59726}\right)\left(1 - \frac{216}{59726}\right)\left(\frac{1}{23430} + \frac{1}{36296}\right)}} =$$

$$\frac{0.00384 - 0.00347}{\sqrt{0.00362 \times 0.99638 \times 0.00007}} = \frac{0.00037}{0.00005} = 0.7363$$

The (right-tail) p-value associated with this under an N(0,1) distribution is very high, namely 0.23077. Thus, we cannot reject the null hypotheses that the two populations have the same success probability.

Bitter taste alleles

The ability or inability to sense a bitter taste from the compound phenylthiocarbamide (PTC) has been hypothesized to directly impact human survival and maintenance of human health. The necessity for foraging societies to accurately discriminate toxic plants, would suggest an ideal situation for strong trait selection. The taste receptor gene *TAS2R38* has therefore been an important marker used to determine the evolution not only of modern humans, but also Neanderthal society[27,28]. Two major *TAS2R38* haplotypes have been described and occur as a

result of three non-synonymous SNPs, namely Ala49Pro (rs713598 G>C), Ala262Val (rs1726866 C>T) and Isl296Val (rs10246939 A>G). PAV (Proline-Alanine-Valine) defines the dominant bitter taste sense haplotype, while AVI (Alanine-Valine-Isoleucine) defines the recessive non-taster haplotype. The predominance of the PAV haplotype in the Bushmen compared to the non-taster AVI haplotype in ABT is suggestive that these alleles may have undergone selective advantage in Bushmen. Further analysis of 12 Bushmen made possible by inclusion of the Ala262Val and Isl296Val variants on the Illumina 1M SNP array identified all o them as PAV for the bitter taste sense contributing alleles. The apparent fixation of these alleles is suggestive of strong selection for acute taste discrimination in a hunter-gatherer, perhaps to avoid toxic plants, but that selection has been relaxed in other populations.

Genes related to hearing

Reportedly, Bushmen have better hearing than Europeans, especially at higher frequencies and also as they age[29,30]. We found Bushmen-specific amino-acid SNPs in two genes in which other SNPs are associated with deafness, *CDH23* and *USH2A* (Supplementary Table 6). Given that altered function of these genes can lead to deafness[31,32], one can speculate that other SNPs in these genes might lead to enhanced hearing. In support of this, we note that the valine in *CDH23* (heterozygous in KB1, rare in non-Bushmen) is the ancestral amino acid, based on comparisons with other primates. Our extensive computational analysis of these SNPs in *CDH23* and *USH2A* can be found at:

http://genomewiki.ucsc.edu/index.php/CDH23_SNPs and
http://genomewiki.ucsc.edu/index.php/USH2A_SNPs.

Experimental testing of this hypothesis may be appropriate. In any case, this illustrates in detail how computational analysis of our data can suggest potential genetic underpinnings for novel Bushmen-specific phenotypes.

Supplementary Tables

Supplementary Table 1. Y-chromosome haplogroup distribution for 20 Bushmen hunters[1] and three European control men from Namibia. Haplogrouping was based on 13 Y-chromosome markers. "ybp" = years before present.

Population Y-chromosome Haplogrouping[3]		A: restricted to Africa (60,000 ybp)		B: restricted to Africa (50,000 ybp)				E: predominant in Africa and African-Americans (emerged via back migration into Africa, 50,000 ybp)				Asian/ Indonesian	Non-African
Haplogroup[2]		A2	A3b1	B2a	B2b	B2b2	B2b4b	E2b	E1b1a	E1b1a4	E1b1b1	O	K-R
1st Marker		M14	M51	M150	M112	M115	M211	M90	M2	M154	M35	M175	M9
2nd Marker		-	-	-	-	-	-	M98	-	-	-	-	-
European	3	0	0	0	0	0	0	0	0	0	0	0	3
Ju/'hoansi	13	**6**	**4**	0	0	0	0	0	1	0	2	0	0
!Kung (Etosha)	4	0	0	0	0	0	0	0	0	0	**4**	0	0
!Kung (Vasekela)	2	1	0	0	0	0	0	0	1	0	0	0	0
Tuu-speaker	1	0	0	0	**1**	0	0	0	0	0	0	0	0

[1] A single individual was selected from each indigenous Namibian hunter-gatherer-identified Y-haplogroup (bold) to undergo extensive sequencing. [2] Population grouping showing predominant representation by the selected haplogroups[33] with classification as per the Y-chromosome consortium (http://ycc.biosci.arizona.edu/) 2008 nomenclature update[4]. [3] Haplogroup continent restriction and estimated emergence times. Haplogroup A sub-groups A2 and A3b1 are seen in Southern Africa, with A3b1 seen exclusively among the Khoisan. Haplogroup B sub-group B2a is seen among Cameroonians, East Africans, and among South African Bantu speakers, while B2b is seen among Central African Pygmies and South African Khoisan. Haplogroup E is similar to D and absent from Africa. E1b1a is an African lineage believed to have expanded from northern African to sub-Saharan and equatorial Africa with the Bantu agricultural expansion. E1b1a is also the most common lineage among African-Americans. Eb1b1 clusters are seen today in Western Europe, Southeast Europe, the Near East, Northeast Africa and Northwest Africa. Haplogroup population definitions are as defined by the International Society of Genetic Genealogy Y-DNA Haplogroup Tree 2009 (http://www.isogg.org/tree/index09.html)[34].

Supplementary Table 2. Basic sequencing statistics for the four Bushmen and the Bantu individual (ABT).

Dataset	Reads	Bases	Mapped bases	CCDS bases
Whole genome, KB1	102,183,3331	35,449,827,671	28,752,706,821	387,254,418
Whole genome, NB1	18,358,065	6,346,320,615	5,628,293,380	67,499,362
Exome, KB1	4,404,906	1,673,892,693	1,553,034,524	394,557,680
Exome, TK1	4,617,978	1,782,031,524	1,662,823,253	427,869,030
Exome, MD8	4,160,900	1,528,147,776	1,434,923,452	364,612,818
Exome, NB1	4,174,479	1,575,488,489	1,472,771,775	370,750,962
Exome, ABT	5,091,760	1,904,113,845	1,777,384,376	479,353,490
Illumina, KB1	539,541,278	81,072,943,456	74,755,457,272[2]	761,387,859
SOLiD, ABT	3,402,047,834	198,473,661,900	78,696,971,148	471,682,954
Illumina, ABT	160,174,952	24,346,592,704	22,940,710,656	218,499,375
Paired-end reads	**Reads**	**Clone coverage**	**Mapped reads**	
KB1	18,851,688	37,834,318,516	3,859,796	

[1]Whole-genome reads for KB1 consist of fragment reads (83,331,226 / 29,165,432,509 / 26,100,525,922 / 283,829,027 reads / bases / mapped bases / CCDS[35] bases), both halves of paired-end reads that are successfully mapped as pairs (12,230,249 / 4,526,728,484 / 1,293,023,468 / 11,098,860), and "rejected" paired-end reads (those that cannot be used as pairs because the linker is either non-existent or is too close to one end to leave a useful half) (6,621,858 / 1,757,666,678 / 1,359,157,431 / 923,26,531).
[2]The numbers for Illumina include reads that map non-uniquely but which are assigned a genomic location at random.

Supplementary Table 3. Statistics from whole exome sequencing.

Sample	Reads[1]	Bases/read[2]	Reads mapped to genome[3]	Reads mapped to exome[4]	Bases mapped to exome	Coverage[5]
KB1	4,404,906	380	4,016,126	2,898,126	394,003,271	15.8X
NB1	4,174,479	377	3,833,171	2,706,077	370,095,481	14.9X
TK1	4,617,978	386	4,239,016	3,057,422	427,178,039	17.2X
MD8	4,160,900	367	3,849,275	2,697,468	364,088,625	14.6X
ABT	5,091,760	374	4,697,586	3,480,207	478,844,708	19.3X

[1] Number of sequencing reads per sample/array.
[2] Average or mean sequencing read length.
[3] Number of reads mapped to the human genome.
[4] Number of reads mapped to the targeted exome (need to use 175,829 as the denominator when calculating this number).
[5] Average coverage per exome.

Supplementary Table 4. Number of SNPs identified for pairs of mitochondrial sequences.

"CRS" = Cambridge Reference Sequence.

	CRS	ABT	KB1	NB1	NB8
CRS	-	100	89	96	95
ABT	100	-	51	84	55
KB1	89	51	-	77	38
NB1	96	84	77	-	75
NB8	95	55	38	75	-

Supplementary Table 5. Human divergence dating using analysis of whole genome mitochondria data

tMRCA Group	M. Ingman et al 2000 *Nature* (Mitochondria) [14]	I. McDougall et al 2005 *Nature* (Geological) [36]	J. P. Noonan et al 2006 *Science* (Genomic) [37]	M. K. Gonder et al 2007 *Mol. Biol. Evol.* (Mitochondria) [38]	R. E. Green et al 2008 *Cell* (Mitochondria)[39]	A. W. Briggs et al 2009 *Science* (Mitochondria) [40]	Our dataset under Relaxed Clock 30 x 10M MCMC chain	Our Dataset under Fixed Clock 27M MCMC chain
H. sapiens sapiens and Neanderthal	NA	NA	706.0 (468.0 – 1015.0)	NA	660.0 (520.0 – 800.0)	NA	Calibrating Point 660.0 (520.0 – 800.0)	Calibrating Point 660.0 (520.0 – 800.0)
H. sapiens sapiens	171.5 (121.5 – 221.5)	> 195.0 (190.0 – 200.0)	NA	194.3 (161.8 – 226.8)	NA	136.1 (94.93 – 178.7)	204.9 (116.8 – 295.7)	237.2 ()
Neanderthal	NA	NA	NA	NA	NA	109.8 (84.63 – 138.5)	130.3 (89.7 – 174.3)	141.2 ()
L0	NA	NA	NA	146.4 (121.3 – 171.5)	NA	NA	158.7 (88.6 – 231.5)	187.9 ()
L0d	NA	NA	NA	106.0 (85.8 – 126.2)	NA	NA	107.2 (56.8 – 159.9)	129.8 ()
Tanzanian L0d	NA	NA	NA	30.6 (12.8 – 48.4)	NA	NA	32.0 (14.6 – 51.6)	36,5 ()
San L0d	NA	NA	NA	90.4 (71.5 – 109.3)	NA	NA	92.8 (47.6 – 139.1)	113.0 ()
L0k, L0f, L0a	NA	NA	NA	139.8 (115.2 – 164.4)	NA	NA	148.2 (NA)	176.9 ()
L0k				70.9 (51.2 – 90.6)			78.6 (37.2 – 122.0)	94.5 ()
L0f, L0a				100.1 (87.6 – 112.6)			118.8 (63.1 – 175.9)	144.0 ()
L0f				94.9 (85.5 – 104.3)			93.8 (46.9 – 139.7)	117.2 ()
L0a				54.6 (48.9 – 60.3)			61.1 (29.2 – 95.1)	71.4 ()
L1, L2, L3, M, N	NA	NA	NA	142.3 (104.1 – 180.5)	NA	NA	172.7 (95.2 – 249.7)	200.9 ()
L3, M, N				94.3 (84.4 – 104.2)			93.3 (50.7 – 136.5)	96.0 ()
Note							Range in parentheses is the 95% HPD interval	
Comments:							GTR + I + Gamma4, Relaxed Clock, Coalescence Expansion Growth, One tMRCA calibration, Six carbon dating data, MCMC chain length 300M, 10% BEAST burn-in. 300030 trees, TreeAnnotator burn-in 10000 trees. Tracer indicate ESS > 600	GTR + I + Gamma4, Strict Clock, Coalescence Expansion Growth, One tMRCA calibration, Six carbon dating data, MCMC chain length 27M, 10% BEAST burn-in. 27000 trees, TreeAnnotator burn-in 1000 trees. Tracer indicates all ESS > 470

*Time Unit in thousands of years.

Supplementary Table 6. Bushman genotypes associated with phenotypes. "Ref." is the human reference assembly.

Gene	NCBI	Build 36	HGMD or dbSNP ID	Ref.	KB1	NB1	MD8	TK1	ABT	known?	Association	PubMed id
ACTN3	chr11	66,084,671	rs1815739:T/C	T	C	C	?	?	C	known	(C;C) possibly increased sprint/power performance; encodes Arg,(C;T) mix of sprinting & endurance muscles,(T;T) possibly increased endurance; T makes a translation terminator	12879365
CDH23	chr10	73,142,571	none	T	T/G	T	T	T	T/G	novel	Encodes a cadherin-like protein in neurosensory epithelium. Variants in *CDH23* are associated with Usher syndrome 1D and deafness. Leu:Leu/Val; Val in ancestral	11090341
CLCNKB	chr1	16,251,312	CM040216	T	A/T	A	?	A	A	known	Increased chloride channel activity, association with T (Thr481Ser)	14675050
CYP2G	chr19	46,260,114	rs10513607	Term	G	G	Term	Term	Term	known	Cytochrome P450, family 2, subfamily g. Gene loss in most humans, but is an active gene in Bushmen. expressed "exclusively" in the olfactory mucosa of mice; involved in steroid metabolism.	18085818
DARC	chr1	157,441,307	rs2814778	T	T	T	T	T/C	C	known	Malaria resistant C-allele	19180233
LCT	chr2	136,325,116	rs4988235	C	C	C	C	C	C	known	Lactase persistence T-allele	11788828
LIPA	chr10	90,997,319	rs1051339	C	C/T	C/T	C	C	C/T	known	Putatively associated with Wolman disease	11441129
SLC24A5	chr15	46,213,776	rs1426654	A	G	G	G	G	G	known	Pale pigmentation A-allele	16357253
TAS2R38	chr7	141,319,073	rs10246939:T/C	T	C	T/C	C	C	T	known	(C;C) can taste bitter,(C;T) can taste bitter,(T;T) unable to taste bitter	12595690
TAS2R38	chr7	141,319,814	rs713598:C/G	C	G	C/G	G	G	C	known	(G;G) can taste bitter,(C;G) can taste bitter,(C;C) unable to taste bitter	12595690
UGT1A3	chr2	234,302,542	CM042128	T	C	T/C	T/C	T/C	T	known	UDP-glucuronosyltransferase activity is higher in the Trp11Arg (121% to 369% compared to major allele, depending on other variants in gene) for estrone metabolism	14986168
USH2A	chr1	213,999,628	none	C	C/T	C/T	C/T	C	C	novel	Mutations in *USH2A* are known to cause Usher syndrome type IIa, which is characterized by deafness and gradual vision loss	9624053
VDR	chr12	46,559,162	CM972826	T	C	T/C	C	C	C	known	Higher bone mineral density, association with C; use of different translation start site	9169350

Supplementary Table 7. Some Gene Ontology categories in which the 6,623 genes with Bushmen-specific amino-acid differences are over- or under-represented.

GO identifier	*p*-value	Over (+) or under (-) abundance	Informal GO category description
0007606	7.40e-25	+	sensory perception of chemical stimulus
0007608	2.22e.23	+	sensory perception of smell
0044255	6.50e-16	+	cellular lipid metabolic process
0019953	3.10e-15	+	sexual reproduction
0007601	6.37e-15	+	visual perception
0031402	1.29e-13	+	sodium ion binding
0007605	2.89e-11	+	sensory perception of sound
0019882	9.40e-11	–	antigen processing and presentation
0019226	6.82e-09	+	transmission of nerve impulse
0007517	7.70e-09	+	muscle organ development
0001501	1.32e-08	+	skeletal system development
0009611	4.33e-07	+	response to wounding
0006954	5.68e-06	+	inflammatory response
0022603	5.50e-05	+	regulation of anatomical structure morphogenesis

Supplementary Table 8. Validated KB1 copy-number variants (CNVs).

geneName	name	chrm	txStart	txEnd	size	KB1 medCN	NA18507 medCN	JDW medCN	YH medCN	WGAC bp	WGAC percent	cn-dir increased	num-probes	mean $\log^2$
KLHL17	NM_198317	1	936,110	941,162	5,053	2.8	1.6	1.7	1.7	0	0.0%	KB1	46	0.133315217
ATAD3C	NM_001039211	1	1,470,336	1,490,805	20,470	4.3	3.2	4.1	3.6	16,121	78.8%	KB1	127	0.040551181
ATAD3B	NM_031921	1	1,492,431	1,516,848	24,418	4.5	3.1	3.4	3.4	24,418	100.0%	KB1	168	-0.010464286
ATAD3A	NM_018188	1	1,532,822	1,555,331	22,510	5.0	3.3	3.8	3.6	22,510	100.0%	KB1	162	0.06916358
CDC2L2	NM_033529	1	1,666,332	1,687,953	21,622	4.5	3.1	3.9	3.2	16,420	75.9%	KB1	152	-0.012404605
ESPN	NM_031475	1	6,419,114	6,455,269	36,156	4.9	3.1	3.1	4.0	31,756	87.8%	KB1	286	0.113879371
NBPF1	NM_017940	1	16,635,718	16,685,288	49,571	49.6	48.0	43.4	46.3	49,533	99.9%	KB1	259	0.050870656
CROCC	NM_014675	1	16,993,751	17,044,780	51,030	5.7	3.0	2.8	3.3	32,413	63.5%	KB1	356	0.211876404
RHD	NM_001127691	1	25,344,297	25,402,252	57,956	4.2	2.6	3.2	3.4	57,956	100.0%	KB1	391	0.327299233
RHCE	NM_138618	1	25,434,057	25,492,679	58,623	4.1	2.6	3.2	3.1	58,449	99.7%	KB1	394	0.254420051
AMY2A	NM_000699	1	103,872,020	103,880,414	8,395	14.0	10.5	5.7	10.8	8,395	100.0%	KB1	65	0.399453846
AMY1A	NM_004038	1	104,004,461	104,013,331	8,871	15.0	11.0	5.7	10.4	8,871	100.0%	KB1	69	0.562384058
PRMT6	NM_018137	1	107,311,451	107,313,956	2,506	3.3	2.2	1.9	2.2	0	0.0%	KB1	24	0.07475
GSTM2	NM_001142368	1	109,922,686	109,938,660	15,975	4.0	2.9	3.1	3.3	10,518	65.8%	KB1	120	0.144604167
GSTM1	NM_000561	1	109,942,460	109,948,408	5,949	4.6	2.6	3.0	2.8	5,948	100.0%	KB1	56	0.82675
IGSF3	NM_001542	1	116,829,073	116,922,356	93,284	7.1	5.9	6.8	5.0	73,003	78.3%	KB1	810	0.006508025
FAM108A3	NM_001080422	1	143,545,025	143,549,782	4,758	20.0	7.4	14.6	11.2	3,724	78.3%	KB1	32	0.247484375
RPTN	NM_001122965	1	148,939,144	148,944,777	5,634	0.9	2.4	2.2	2.8	0	0.0%	NA18507	56	-0.208571429
MSTO1	NM_018116	1	152,393,080	152,397,830	4,751	2.8	4.0	3.7	3.9	4,751	100.0%	NA18507	46	-0.153967391
FCER1G	NM_004106	1	157,998,160	158,002,111	3,952	0.0	1.7	1.6	1.6	0	0.0%	NA18507	30	-0.187433333
FCGR2A	NM_001136219	1	158,288,260	158,302,414	14,155	3.1	4.2	4.3	3.8	3,867	27.3%	NA18507	116	-0.288969828
FCGR3B	NM_000570	1	158,324,606	158,332,855	8,250	3.2	4.4	4.1	4.0	0	0.0%	NA18507	68	-0.470294118
FCGR3A	NM_001127593	1	158,324,606	158,333,468	8,863	3.1	4.4	3.9	3.8	0	0.0%	NA18507	73	-0.45589726
FCGR2C	NM_001005410	1	158,364,613	158,375,530	10,918	2.9	4.0	4.0	3.5	1,112	10.2%	NA18507	95	-0.462821053
CFHR3	NM_021023	1	193,475,587	193,494,529	18,943	3.1	2.0	5.0	3.8	12,709	67.1%	KB1	99	0.437929293
CFHR1	NM_002113	1	193,520,518	193,532,973	12,456	2.8	1.6	3.8	2.8	12,455	100.0%	KB1	90	0.458661111
MRPL55	NM_181465	1	224,601,115	224,603,748	2,634	4.6	2.0	2.7	2.2	0	0.0%	KB1	19	0.059
SYT15	NM_031912	10	46,378,534	46,390,607	12,074	6.8	3.8	4.0	4.3	6,052	50.1%	KB1	101	0.087455446
GPRIN2	NM_014696	10	46,413,552	46,420,573	7,022	4.7	3.5	4.2	3.9	0	0.0%	KB1	66	0.054537879
FAM22A	NM_001099338	10	88,975,185	88,984,713	9,529	16.3	9.4	11.6	11.1	9,529	100.0%	KB1	89	0.09191573
FAM22D	NM_001009610	10	89,107,457	89,120,432	12,976	15.4	9.1	11.5	11.1	12,976	100.0%	KB1	121	0.078115702
HPS6	NM_024747	10	103,815,137	103,817,782	2,646	3.3	2.1	2.4	1.9	0	0.0%	KB1	26	0.059326923
CYP2E1	NM_000773	10	135,229,748	135,241,501	11,754	4.5	2.0	2.5	2.1	0	0.0%	KB1	101	0.561806931
SYCE1	NM_130784	10	135,256,285	135,271,757	15,473	3.6	1.9	1.7	1.9	1,887	12.2%	KB1	116	0.508306034
DUX4	NM_033178	10	135,372,560	135,380,764	8,205	185.8	96.6	247.8	195.7	8,205	100.0%	KB1	58	0.424715517
NLRP6	NM_138329	11	268,570	275,303	6,734	2.9	1.8	2.0	1.8	0	0.0%	KB1	62	0.016080645
EFCAB4A	NM_173584	11	817,585	821,991	4,407	2.7	1.5	1.3	1.7	0	0.0%	KB1	40	0.083725
MUC6	NM_005961	11	1,002,824	1,026,706	23,883	3.1	1.8	2.1	1.7	0	0.0%	KB1	226	0.021827434
CHRNA10	NM_020402	11	3,643,393	3,649,190	5,798	0.8	1.9	1.8	1.8	0	0.0%	NA18507	52	-0.179009615
KCNJ11	NM_000525	11	17,363,374	17,366,782	3,409	4.4	2.3	3.4	3.1	0	0.0%	KB1	28	0.134196429
TIGD3	NM_145719	11	64,878,858	64,881,658	2,801	3.8	1.9	2.2	2.2	0	0.0%	KB1	22	0.056840909
UNC93B1	NM_030930	11	67,515,151	67,528,169	13,019	3.3	2.2	2.0	2.1	5,071	39.0%	KB1	92	0.017478261
FAM86C	NM_152563	11	71,176,205	71,189,928	13,724	23.7	16.3	18.2	18.3	13,724	100.0%	KB1	84	0.041767857
CRYAB	NM_001885	11	111,284,560	111,287,683	3,124	0.9	2.2	1.8	2.1	0	0.0%	NA18507	30	-0.200516667
PATE1	NM_138294	11	125,121,398	125,124,952	3,555	0.8	1.8	1.9	1.7	0	0.0%	NA18507	34	-0.208338235
PRB1	NM_199353	12	11,396,024	11,399,791	3,768	3.4	12.2	6.5	10.8	3,768	100.0%	NA18507	29	-0.34262069
PRB2	NM_006248	12	11,435,743	11,439,765	4,023	4.0	6.8	6.0	6.2	4,023	100.0%	NA18507	28	-0.292178571
TUBA3C	NM_006001	13	18,645,920	18,653,936	8,017	7.3	4.9	6.3	5.3	0	0.0%	KB1	56	0.0205
PRR20	NM_198441	13	56,639,332	56,642,353	3,022	41.2	22.4	27.9	10.8	3,022	100.0%	KB1	21	0.464
DHRS4L2	NM_198083	14	23,527,867	23,545,459	17,593	4.3	5.5	5.5	5.4	17,592	100.0%	NA18507	115	-0.14183913
DHRS4L1	NM_001082488	14	23,575,550	23,590,420	14,871	3.8	4.9	5.1	4.7	297	2.0%	NA18507	105	-0.134119048
SDR39U1	NM_020195	14	23,978,814	23,981,847	3,034	1.0	2.2	2.7	2.1	0	0.0%	NA18507	27	-0.182685185
ACOT1	NM_001037161	14	73,073,681	73,080,251	6,571	2.5	1.3	1.3	2.0	6,571	100.0%	KB1	38	0.393486842
LOC727832	NM_001145004	15	18,997,108	19,007,128	10,021	27.6	26.0	27.5	26.3	10,021	100.0%	KB1	45	0.018655556
LOC283767	NM_001001413	15	20,287,610	20,297,366	9,757	26.0	22.1	25.7	26.1	9,757	100.0%	KB1	45	0.045244444
NIPA1	NM_001142275	15	20,594,722	20,638,284	43,563	2.0	0.9	2.0	1.8	0	0.0%	KB1	242	0.362549587
GOLGA8E	NM_001012423	15	20,986,537	20,999,864	13,328	35.5	34.5	35.7	37.9	13,328	100.0%	KB1	47	0.075031915
CHRFAM7A	NM_148911	15	28,440,735	28,473,156	32,422	5.8	3.9	4.7	4.0	32,422	100.0%	KB1	226	-0.008878319
GOLGA8A	NM_181077	15	32,458,564	32,487,180	28,617	6.9	10.0	8.4	8.6	28,617	100.0%	NA18507	196	-0.244607143
TEX9	NM_198524	15	54,444,936	54,525,363	80,428	1.9	0.9	1.7	1.7	0	0.0%	KB1	435	0.198298851
GOLGA6	NM_001038640	15	72,149,251	72,161,944	12,694	16.7	13.2	17.2	16.8	12,694	100.0%	KB1	80	0.21210625
RHOT2	NM_138769	16	658,134	664,171	6,038	2.7	1.6	1.6	1.6	0	0.0%	KB1	54	0.124666667
STUB1	NM_005861	16	670,116	672,768	2,653	3.0	1.9	1.4	2.0	0	0.0%	KB1	22	0.062727273
JMJD8	NM_001005920	16	671,668	674,440	2,773	3.3	2.2	2.0	1.8	0	0.0%	KB1	23	0.107978261
WDR24	NM_032259	16	674,703	680,401	5,699	2.8	1.8	2.0	1.9	0	0.0%	KB1	51	0.085029412
GNG13	NM_016541	16	788,042	790,734	2,693	2.9	1.8	1.5	1.7	0	0.0%	KB1	25	0.03934
IGFALS	NM_004970	16	1,780,422	1,783,710	3,289	3.1	1.8	1.5	1.7	0	0.0%	KB1	32	0.089390625
PKD1	NM_000296	16	2,078,712	2,125,900	47,189	7.2	3.4	6.6	4.4	38,481	81.5%	KB1	385	0.051514286
PRSS33	NM_152891	16	2,773,955	2,776,709	2,755	2.8	1.7	0.9	1.2	0	0.0%	KB1	25	0.06256
ALG1	NM_019109	16	5,061,811	5,077,379	15,569	10.9	8.8	10.0	8.6	9,707	62.3%	KB1	101	0.041673267
FAM86A	NM_201598	16	5,074,303	5,087,790	13,488	21.0	13.6	16.0	16.9	13,488	100.0%	KB1	80	0.05915625
PDXDC1	NM_015027	16	14,976,334	15,039,053	62,720	3.9	5.3	5.0	3.9	55,935	89.2%	NA18507	384	-0.21915625
ORAI3	NM_152288	16	30,867,906	30,873,759	5,854	2.8	1.8	2.1	2.1	0	0.0%	KB1	43	0.03355814
SLC5A2	NM_003041	16	31,401,940	31,409,592	7,653	3.1	1.9	2.3	1.9	0	0.0%	KB1	63	0.094531746
TP53TG3	NM_016212	16	33,112,481	33,115,680	3,200	16.5	6.9	15.9	6.1	3,200	100.0%	KB1	29	0.286844828
PDPR	NM_017990	16	68,705,030	68,752,685	47,656	3.4	5.1	4.0	4.0	35,926	75.4%	NA18507	261	-0.358015326
MRCL	NM_173619	16	68,765,429	68,778,297	12,869	8.8	6.2	6.2	6.1	12,869	100.0%	KB1	95	0.040868421
CTRB2	NM_001025200	16	73,795,496	73,798,573	3,078	4.4	2.3	3.3	2.6	1,533	49.8%	KB1	27	0.107055556
CTRB1	NM_001906	16	73,810,385	73,816,322	5,938	3.7	2.2	3.1	2.6	1,533	25.8%	KB1	41	0.057560976
SLC16A11	NM_153357	17	6,885,673	6,887,966	2,294	3.3	1.7	2.2	1.4	0	0.0%	KB1	17	0.051205882

FLJ25006	NM_144610	17	23,959,109	23,965,338	6,230	0.7	2.2	1.5	2.2	0	0.0%	NA18507	49	-0.216612245
ARL17	NM_001039083	17	41,989,936	42,012,375	22,440	3.8	1.6	3.9	5.2	22,440	100.0%	KB1	121	0.380884298
NPEPPS	NM_006310	17	42,963,443	43,055,641	92,199	3.5	8.3	4.4	3.5	62,993	68.3%	NA18507	458	-0.291865721
GIP	NM_004123	17	44,390,917	44,400,954	10,038	1.4	2.7	2.0	3.0	0	0.0%	NA18507	43	-0.143290698
POLRMT	NM_005035	19	568,223	584,568	16,346	3.0	2.0	2.5	2.3	0	0.0%	KB1	118	0.037338983
KISS1R	NM_032551	19	868,342	872,015	3,674	3.0	1.7	3.4	1.6	0	0.0%	KB1	31	0.094887097
NDUFS7	NM_024407	19	1,334,883	1,346,588	11,706	2.8	1.8	1.8	1.7	0	0.0%	KB1	86	0.049627907
FAM108A1	NM_031213	19	1,827,975	1,836,518	8,544	4.0	1.9	3.3	2.0	4,828	56.5%	KB1	74	0.115695946
ZNF555	NM_152791	19	2,792,482	2,805,033	12,552	1.4	2.7	4.0	2.9	0	0.0%	NA18507	75	-0.182393333
FUT5	NM_002034	19	5,816,838	5,821,551	4,714	5.2	2.7	3.3	3.1	0	0.0%	KB1	29	0.033327586
MBD3L2	NM_144614	19	7,000,351	7,002,746	2,396	10.1	7.0	8.1	8.0	2,396	100.0%	KB1	21	0.408261905
EPOR	NM_000121	19	11,349,475	11,356,019	6,545	3.1	2.1	2.3	2.0	0	0.0%	KB1	46	0.036771739
ZNF439	NM_152262	19	11,837,844	11,841,306	3,463	5.4	7.8	7.7	7.7	0	0.0%	NA18507	30	-0.187483333
ZNF700	NM_144566	19	11,896,900	11,922,577	25,678	2.5	4.2	3.7	4.3	0	0.0%	NA18507	139	-0.190111511
RASAL3	NM_022904	19	15,423,438	15,436,382	12,945	0.8	1.8	1.2	1.6	0	0.0%	NA18507	85	-0.151923529
ISYNA1	NM_016368	19	18,406,625	18,409,943	3,319	3.4	2.0	2.9	2.1	0	0.0%	KB1	27	0.102037037
FCGBP	NM_003890	19	45,045,803	45,132,373	86,571	6.3	4.5	4.1	4.3	31,438	36.3%	KB1	620	-0.032360484
CYP2A6	NM_000762	19	46,041,283	46,048,192	6,910	6.6	4.7	4.6	4.4	6,910	100.0%	KB1	62	0.094048387
CEACAM5	NM_004363	19	46,904,370	46,926,276	21,907	3.1	4.5	4.5	4.5	0	0.0%	NA18507	171	-0.133769006
CEACAM8	NM_001816	19	47,776,235	47,790,922	14,688	3.6	5.2	5.6	4.9	0	0.0%	NA18507	112	-0.127348214
PSG3	NM_021016	19	47,917,635	47,936,508	18,874	10.3	11.4	10.2	9.2	18,874	100.0%	NA18507	139	-0.124496403
PSG8	NM_182707	19	47,950,225	47,961,671	11,447	9.9	13.3	12.6	11.2	11,447	100.0%	NA18507	93	-0.194989247
PSG1	NM_006905	19	48,063,198	48,075,711	12,514	10.3	13.4	13.0	9.9	12,514	100.0%	NA18507	100	-0.18997
PSG6	NM_002782	19	48,099,608	48,113,829	14,222	8.5	13.1	13.1	9.6	14,222	100.0%	NA18507	111	-0.161837838
PSG7	NM_002783	19	48,120,124	48,133,170	13,047	10.0	12.3	12.1	9.7	13,047	100.0%	NA18507	109	-0.162458716
PSG11	NM_203287	19	48,203,649	48,222,471	18,823	10.3	13.1	12.4	9.9	18,823	100.0%	NA18507	148	-0.11710473
PSG5	NM_002781	19	48,363,735	48,382,528	18,794	9.0	11.3	10.9	9.4	18,794	100.0%	NA18507	147	-0.146755102
PSG4	NM_002780	19	48,388,696	48,401,630	12,935	10.4	13.1	13.4	10.4	12,935	100.0%	NA18507	111	-0.25104955
PSG9	NM_002784	19	48,449,275	48,465,522	16,248	10.7	13.1	13.3	10.1	16,248	100.0%	NA18507	129	-0.20755814
SEPW1	NM_003009	19	52,973,654	52,979,751	6,098	1.3	2.6	2.0	3.7	0	0.0%	NA18507	43	-0.163174419
RPS11	NM_001015	19	54,691,446	54,694,756	3,311	1.9	3.1	3.2	2.4	0	0.0%	NA18507	26	-0.175442308
RFPL4A	NM_001145014	19	60,962,319	60,966,351	4,033	7.2	5.4	5.3	5.0	4,033	100.0%	KB1	34	0.249617647
RHOB	NM_004040	2	20,568,463	20,570,828	2,366	2.7	1.7	2.9	1.8	0	0.0%	KB1	23	0.075108696
TCF23	NM_175769	2	27,283,653	27,287,384	3,732	3.3	2.1	1.9	2.1	0	0.0%	KB1	29	0.013982759
C2orf78	NM_001080474	2	73,922,971	73,955,929	32,959	2.6	7.2	9.5	14.1	26,245	79.6%	NA18507	186	-0.453905914
TEKT4	NM_144705	2	94,959,106	94,964,442	5,337	11.0	6.2	7.1	7.8	5,337	100.0%	KB1	49	0.111010204
SMPD4	NM_017951	2	130,625,210	130,655,924	30,715	4.7	3.4	3.8	3.9	30,715	100.0%	KB1	222	0.053752252
C2orf27	NM_013310	2	132,313,796	132,358,709	44,914	11.5	9.8	8.7	10.7	44,914	100.0%	KB1	312	0.0876875
MGC50273	NM_214461	2	132,386,266	132,392,966	6,701	33.3	27.9	33.3	31.7	6,701	100.0%	KB1	44	0.114090909
CHPF	NM_024536	2	220,229,174	220,233,992	4,819	3.1	2.0	2.4	2.3	0	0.0%	KB1	45	0.065577778
ALPP	NM_001632	2	233,068,853	233,073,102	4,250	5.2	3.2	3.8	3.7	4,250	100.0%	KB1	38	0.040736842
ALPPL2	NM_031313	2	233,097,057	233,100,930	3,874	5.2	3.5	3.8	4.2	3,874	100.0%	KB1	37	0.039837838
ALPI	NM_001631	2	233,146,338	233,150,247	3,910	4.0	2.9	3.8	3.2	0	0.0%	KB1	39	0.063166667
NDUFA10	NM_004544	2	240,620,146	240,684,788	64,643	3.0	1.8	2.0	1.9	0	0.0%	KB1	553	0.294776673
RNPEPL1	NM_018226	2	241,228,094	241,238,131	10,038	2.6	1.6	1.8	1.9	0	0.0%	KB1	97	0.02164433
AQP12A	NM_198998	2	241,351,252	241,357,889	6,638	4.1	2.7	2.8	3.0	6,638	100.0%	KB1	63	0.146007937
GNRH2	NM_178331	20	2,972,268	2,974,391	2,124	3.6	2.2	2.2	2.2	0	0.0%	KB1	20	0.062875
THBD	NM_000361	20	22,974,271	22,978,301	4,031	2.7	1.6	1.8	1.9	0	0.0%	KB1	40	0.08135
CST4	NM_001899	20	23,614,277	23,617,662	3,386	5.7	4.0	4.2	4.9	3,386	100.0%	KB1	35	0.073871429
C20orf134	NM_001024675	20	31,717,965	31,719,991	2,027	3.4	2.0	2.9	2.5	0	0.0%	KB1	19	0.093526316
SEMG1	NM_003007	20	43,269,088	43,271,822	2,735	2.5	4.1	3.2	3.4	0	0.0%	NA18507	26	-0.200826923
SEMG2	NM_003008	20	43,283,424	43,286,512	3,089	2.3	4.9	5.0	4.0	0	0.0%	NA18507	30	-0.161666667
NEURL2	NM_080749	20	43,950,674	43,953,308	2,635	4.4	1.9	2.0	1.9	0	0.0%	KB1	19	0.074368421
THAP7	NM_001008695	22	19,678,615	19,680,958	2,344	3.7	2.0	3.2	1.7	0	0.0%	KB1	23	0.133369565
LOC51233	NM_016449	22	22,275,194	22,299,041	23,848	3.2	4.4	4.0	4.0	15,467	64.9%	NA18507	185	-0.135435135
DDT	NM_001355	22	22,638,108	22,646,573	8,466	3.4	1.8	3.3	3.6	8,056	95.2%	KB1	60	0.335975
GSTT2	NM_000854	22	22,646,868	22,650,660	3,793	3.6	2.0	2.8	3.6	3,793	100.0%	KB1	30	0.38805
GSTT1	NM_000853	22	22,700,693	22,708,838	8,146	0.0	1.2	1.3	0.4	0	0.0%	NA18507	54	-0.807518519
GGT1	NM_001032365	22	23,328,209	23,349,526	21,318	13.2	7.2	9.2	6.3	21,318	100.0%	KB1	137	0.181193431
APOBEC3B	NM_004900	22	37,702,905	37,713,283	10,379	3.3	2.2	2.6	3.1	10,290	99.1%	KB1	91	0.240824176
RRP7A	NM_015703	22	41,233,073	41,240,306	7,234	4.0	2.7	3.1	3.1	7,234	100.0%	KB1	54	0.200611111
LMF2	NM_033200	22	49,231,524	49,236,257	4,734	3.8	1.9	2.4	1.9	0	0.0%	KB1	41	0.035780488
MST1	NM_020998	3	49,696,385	49,701,200	4,816	12.7	6.0	11.5	10.7	4,776	99.2%	KB1	47	2.68E-01
AMIGO3	NM_198722	3	49,729,969	49,732,127	2,159	3.5	1.7	2.7	2.1	0	0.0%	KB1	22	0.115022727
CISH	NM_013324	3	50,618,890	50,624,266	5,377	3.8	2.1	2.6	2.4	0	0.0%	KB1	52	0.027278846
TLR9	NM_017442	3	52,230,138	52,235,219	5,082	4.0	2.1	2.0	2.5	0	0.0%	KB1	47	0.0045
FAM157A	NM_001145248	3	199,367,547	199,396,038	28,492	13.0	9.9	11.0	8.3	28,492	100.0%	KB1	152	-0.012078947
SLC26A1	NM_213613	4	971,277	977,054	5,778	3.2	1.8	2.6	2.0	0	0.0%	KB1	55	0.068145455
DRD5	NM_000798	4	9,459,527	9,461,902	2,376	19.8	8.9	10.4	12.3	2,376	100.0%	KB1	23	0.156347826
UGT2B15	NM_001076	4	69,693,104	69,717,150	24,047	2.3	4.1	4.5	2.6	24,047	100.0%	NA18507	139	-0.308435252
UGT2B11	NM_001073	4	70,246,807	70,261,209	14,403	5.8	8.9	9.0	7.2	14,403	100.0%	NA18507	112	-0.123209821
FRG2	NM_001005217	4	191,320,672	191,323,561	2,890	10.6	9.0	12.9	9.7	2,890	100.0%	KB1	24	0.055666667
MGC29506	NM_016459	5	138,751,157	138,753,504	2,348	3.1	1.7	1.9	1.8	0	0.0%	KB1	20	0.078725
ZNF300	NM_052860	5	150,254,157	150,264,584	10,428	1.5	2.5	2.6	2.2	1,060	10.2%	NA18507	89	-0.15955618
FGFR4	NM_022963	5	176,449,157	176,457,730	8,574	3.1	2.0	2.0	2.2	0	0.0%	KB1	79	0.026537975
HSPA1A	NM_005345	6	31,891,270	31,893,698	2,429	5.9	4.0	5.7	5.1	2,177	89.6%	KB1	23	0.059934783
TREML1	NM_178174	6	41,225,322	41,230,048	4,727	1.2	2.3	2.5	2.4	0	0.0%	NA18507	37	-0.175081081
GSTA1	NM_145740	6	52,764,138	52,776,623	12,486	5.0	6.5	6.1	5.9	12,486	100.0%	NA18507	111	-0.115342342
GSTA5	NM_153699	6	52,804,502	52,818,852	14,351	4.5	5.6	5.4	5.0	14,351	100.0%	NA18507	117	-0.123858974
MARCKS	NM_002356	6	114,285,220	114,291,345	6,126	1.4	2.8	2.3	2.5	2,419	39.5%	NA18507	40	-0.286275
CYP2W1	NM_017781	7	796,076	802,517	6,442	3.1	2.1	2.3	2.0	0	0.0%	KB1	54	0.085592593
TMEM184A	NM_001097620	7	1,355,112	1,369,307	14,196	3.3	2.1	2.1	2.0	0	0.0%	KB1	116	0.091672414
KIAA0415	NM_014855	7	4,588,505	4,604,638	16,134	3.0	2.0	2.1	2.0	0	0.0%	KB1	117	0.069333333
NCF1	NM_000265	7	73,632,960	73,648,309	15,350	5.7	4.4	5.1	4.8	15,350	100.0%	KB1	82	0.061152439

PMS2L5	NM_174930	7	73,751,552	73,766,505	14,954	22.0	18.7	17.9	16.0	14,954	100.0%	KB1	23	0.242782609
LOC442590	NM_001099435	7	74,768,950	74,778,279	9,330	40.9	33.4	35.6	32.2	9,330	100.0%	KB1	20	0.052
DTX2	NM_020892	7	75,735,623	75,779,963	44,341	4.9	3.4	3.9	2.7	44,341	100.0%	KB1	310	0.007883871
UPK3B	NM_182684	7	75,784,396	75,801,848	17,453	3.4	2.1	2.4	1.6	17,453	100.0%	KB1	82	0.109890244
LOC100132832	NM_001129851	7	76,313,448	76,327,006	13,559	24.0	22.6	21.7	19.8	13,559	100.0%	KB1	17	0.113088235
CYP3A4	NM_017460	7	98,999,255	99,026,459	27,205	2.6	3.7	3.4	3.4	27,205	100.0%	NA18507	203	-0.129889163
STAG3	NM_012447	7	99,420,189	99,456,661	36,473	1.9	3.2	2.7	2.7	18,414	50.5%	NA18507	229	-0.130454148
ACHE	NM_000665	7	100,132,267	100,138,192	5,926	3.5	2.0	2.8	2.0	0	0.0%	KB1	43	0.100093023
POLR2J	NM_006234	7	101,707,270	101,713,101	5,832	11.5	8.5	7.8	10.4	4,996	85.7%	KB1	43	0.159523256
RASA4	NM_001079877	7	101,813,883	101,851,140	37,258	11.1	6.1	6.5	7.8	37,258	100.0%	KB1	225	0.253435556
POLR2J2	NM_032959	7	101,871,425	101,906,133	34,709	19.7	12.1	12.9	13.2	34,709	100.0%	KB1	143	0.170545455
ZYX	NM_001010972	7	142,595,197	142,605,039	9,843	3.3	2.1	2.5	2.3	0	0.0%	KB1	87	0.008074713
FLJ43692	NM_001003702	7	143,321,325	143,330,384	9,060	8.8	6.0	6.4	8.5	9,051	99.9%	KB1	75	0.057346667
ARHGEF5	NM_005435	7	143,490,137	143,515,372	25,236	6.2	4.0	5.0	6.1	21,888	86.7%	KB1	211	0.136881517
DEFA1	NM_004084	8	6,841,698	6,844,122	2,425	12.6	7.6	9.1	6.1	2,425	100.0%	KB1	23	0.314173913
DEFA3	NM_005217	8	6,860,805	6,863,226	2,422	12.0	7.6	8.6	6.2	0	0.0%	KB1	24	0.324520833
SPAG11A	NM_001081552	8	7,742,812	7,758,729	15,918	5.6	2.9	1.9	4.2	15,918	100.0%	KB1	134	0.410011194
FAM86B2	NM_001137610	8	12,327,497	12,338,223	10,727	27.1	16.7	20.2	20.8	10,727	100.0%	KB1	67	0.123007463
REXO1L1	NM_172239	8	86,755,947	86,762,978	7,032	272.4	129.9	183.7	134.9	7,032	100.0%	KB1	50	0.36707
CYP11B1	NM_001026213	8	143,950,777	143,958,238	7,462	3.7	2.6	2.8	3.1	6,656	89.2%	KB1	72	0.040833333
VPS28	NM_016208	8	145,619,808	145,624,735	4,928	3.3	2.0	2.1	2.0	0	0.0%	KB1	43	0.049093023
PPP1R16A	NM_032902	8	145,692,917	145,698,311	5,395	2.6	1.6	1.8	1.9	0	0.0%	KB1	52	0.008
LRRC14	NM_014665	8	145,714,199	145,721,365	7,167	3.1	2.0	1.8	2.0	0	0.0%	KB1	65	0.027130769
WASH1	NM_182905	9	4,511	19,739	15,229	26.1	16.0	25.6	19.8	15,229	100.0%	KB1	133	0.16081203
AQP7	NM_001170	9	33,374,949	33,392,517	17,569	14.1	9.3	10.5	9.4	17,569	100.0%	KB1	139	0.003571942
FAM75A1	NM_001085452	9	39,657,015	39,663,247	6,233	13.0	11.1	13.6	11.5	6,233	100.0%	KB1	49	0.063295918
FAM22F	NM_017561	9	94,160,033	94,170,481	10,449	11.3	7.5	9.0	8.6	10,449	100.0%	KB1	84	0.076113095
SET	NM_001122821	9	128,525,488	128,538,229	12,742	3.5	4.7	4.0	4.1	1,752	13.7%	NA18507	81	-0.170783951
FBXW5	NM_018998	9	137,110,725	137,115,010	4,286	3.1	1.8	2.1	1.8	0	0.0%	KB1	37	0.151310811

Validation was based on array CGH (comparative genomic hybridization) with the NA18507 (Yoruban) genome sequence[41]. "tx" = transcription, "medCN" = nedian copy number, "WGAC" = whole genome assembly comparison.

Supplementary Table 9. Mitochondrial haplogroups[42] based on four informative Illumina 1M Duo mitochondrial SNPs.

	KB1	NB1	TK1	MD8	ABT
MitoG1440A	G	A	A	A	G
MitoG2708A	G	A	A	A	A
MitoG15931A	G	A	A	A	G
MitoG16130A	G	A	A	A	G

Supplementary Table 10. Markers for NB1 and TK1 that define Y-haplogroup A[1].

SNP ID	Position[2]	Name	Haplogroup	Change[3]	NB1	TK1
rs3897	17080420	M6	A2	T>C	T	C
rs3905	20181656	M14	A2	T>C	T	C
rs2032633	20328114	M49	A2	T>C	T	C
rs2032638	20353835	M71	A2	C>T	C	T
rs2032664	14036089	M212	A2	C>A	C	C[#]
rs9341312	21151116	P247	A2	T>A	T	A
rs9341314	21151209	P248	A2	G>T	G	T
rs2032603	13477921	M190	A3b	A>G	G	A

[1]Identified using genotyping array data and/or genome sequencing data. [2]Position and [3]substitution based on NCBI Build 36 (hg18 reference sequence). [#]Genotype according to Illumina 1M array denotes TK1 as not being in the A2 haplogroup as per the M212 marker. This discordance may indicate genotyping error or a *de novo* mutation in this individual.

Supplementary Table 11. Markers for KB1 that define Y-haplogroup B[1].

SNP ID	Position[2]	Name	Haplogroup	Change[3]	KB1
rs2032599	13360948	M181	B	T>C	C
rs9341290	13529972	P85	B	T>C	C
-	13359973	P90	B	C>T	T
rs2032601	13378470	M182	B2	C>T	T
-	20227347	M112	B2b	C>T (G>A*)	T
rs2032662	13523656	M192	B2b	C>T	T
-	21906455	50f2(P)	B2b	G>C	G
-	6828265	P6	B2b1	G>C	C

[1]Identified using genotyping array data and/or genome sequencing data. [2]Position and [3]substitution based on NCBI Build 36 (hg18 reference sequence). *Strand orientation as per ref. 4.

Supplementary Table 12. Markers for ABT and MD8 that define Y-haplogroup E[1].

SNP ID	Position[2]	Name	Haplogroup	Change[3]	ABT	MD8
rs9786489	10461457 *	P167	DE	G>T	T	T
rs9786634	13174651 *	P152	E	G>C	C	C
rs9786357	18009501 *	P154	E	G>T	T	T
rs9786301	14847931 *	P155	E	G>A	A	A
rs17842518	21853359 *	P171	E	G>T	T	T
rs9786191	13313471 *	P175	E	G>A	A	A
rs16980473	12669846	P177	E1b	C>T	T	T
rs9786105	7461836 *	P178	E1b1	G>A	A	A
-	20071555	P1	E1b1a	C>T	T	C
rs16980394	17745841 *	P182	E1b1a	G>A	A	G
rs16981297	8835178	P293	E1b1a	G>A	A	G
rs2032598	13359735	M180 P88	E1b1a	T>C	C	T
rs9786252	2971033 *	-	E1b1a	G>A	A	G
rs768983	6878291 *	-	E1b1a	G>A (C>T*)	A	G
rs9786574	8647013 *	-	E1b1a	C>T	T	C
rs16980754	8806440 *	-	E1b1a	C>T	T	C
rs9785753	13176589 *	-	E1b1a	C>T	T	C
rs9786100	13824441 *	-	E1b1a	T>C	C	T
rs9786135	17246254 *	-	E1b1a	C>T	T	C
rs16980561	21081419 *	-	E1b1a	A>G	G	A
rs16980435	21531096 *	-	E1b1a	C>T	T	C
rs9785875	22788755 *	-	E1b1a	T>A	A	T
rs1971755	15087466 *	-	E1b1a	A>G (T>C*)	G	A
rs16980457	15222712 *	-	E1b1a	G>T	T	G
rs16980588	14763088 *	U175	E1b1a8	G>A	A	G
rs16980502	15804352 *	U209	E1b1a8a	C>T	T	C
rs16980558	14088609	P277	E1b1a8a	A>G	G	A
rs7067418	85227053	P278	E1b1a8a	G>A	A	G
-	20201091	M35	E1b1b1	G>C	G	C
rs2032640	20351960	M81	E1b1b1b	C>T	C	C
rs2032613	20391026	M107	E1b1b1b1	A>G	A	A

[1]Identified using genotyping array data and/or genome sequencing data. [2]Position and [3]substitution based on NCBI Build 36 (hg18 reference sequence). *Nucleotide position or strand orientation as per ref. 4.

Supplementary Table 13. 5-by-5 F*st* (fixation index) table depicting relationships among the five men using genome-wide SNP analysis.

		KB1	NB1	TK1	MD8	ABT
KB1	Fst x1000	0	21	24	22	80
	SD x1M	-	*4372*	*4785*	*4536*	*4902*
NB1	Fst x1000	21	0	-7	6	91
	SD x1M	*4372*	-	*5580*	*4398*	*4790*
TK1	Fst x1000	24	-7	0	16	88
	SD x1M	*4785*	*5580*	-	*4934*	*4916*
MD8	Fst x1000	22	6	16	0	61
	SD x1M	*4536*	*4398*	*4934*	-	*4867*
ABT	Fst x1000	80	91	88	61	0
	SD x1M	*4902*	*4790*	*4916*	*4867*	-

Supplementary Table 14. Evidence for gene-flow between ancestors of ABT and KB1. An excess of sites at which ABT and KB1 share a derived allele relative to another genome, X, is a signal of admixture (see Ref. 43 for details). We searched for such an excess at 39,473 neutral, freely recombining, autosomal loci, each 1kb in size. Six different genomes were used in place of X. Positive values of the test statistic ($C_{abt\text{-}x}$) indicate potential admixture between ancestors of KB1 and ABT. Statistical significance was assessed using a permutation test, as described in Ref. 43.

X	Population	$C_{abt\text{-}x}$ [a]	μ_0 [b]	σ_0 [c]	p [d]
NA18507	Yoruban	208.13	0.06	50.88	**0.00002**
NA19240	Yoruban	166.75	-0.01	46.82	**0.00018**
NA12891	European	62.88	0.23	52.83	0.11735
NA12892	European	84.88	0.11	52.12	0.05218
Korean	Korean	117.50	0.22	52.40	**0.01202**
Chinese	Chinese	59.63	0.29	53.39	0.13180

[a]Observed value of test statistic, based on real data (see text).
[b]Mean of null distribution, as assessed by permutation test.
[c]Standard deviation of null distribution, as assessed by permutation test.
[d]Empirical one-sided *p*-value: fraction of 100,000 permuted data sets having test statistics at least as large as $C_{abt\text{-}x}$. Values of $p < 0.05$ are highlighted in bold.

Supplementary Table 15. KB1 genotypes at various unstable microsatellite loci. Loci are identified in Pearson et al[11]. Only alleles supported by at least two reads are presented here. "Ref." is the human reference genome (NCBI Build 36).

Locus	Normal range	Disease range	Ref.	KB1
DRPLA	7-25	49-88	15	9
SCA10	10-22	800-4500	14	13
SCA12	7-45	55-78	10	13
SCA6	4-18	20-29	13	8/11

Supplementary Figures

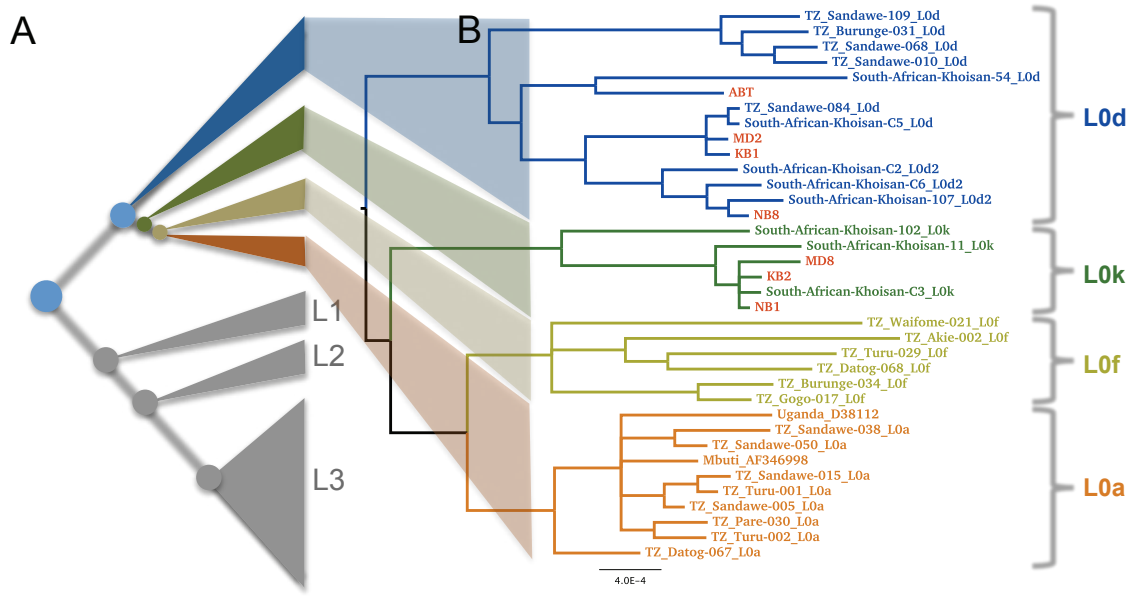

Supplementary Figure 1A. Phylogenetic trees.
(A) Schematic tree of mitochondrial human haplogroups. (B) Bayesian phylogenetic tree of complete mitochondrial genomes from haplogroup L0. Individuals from this study are highlighted in red.

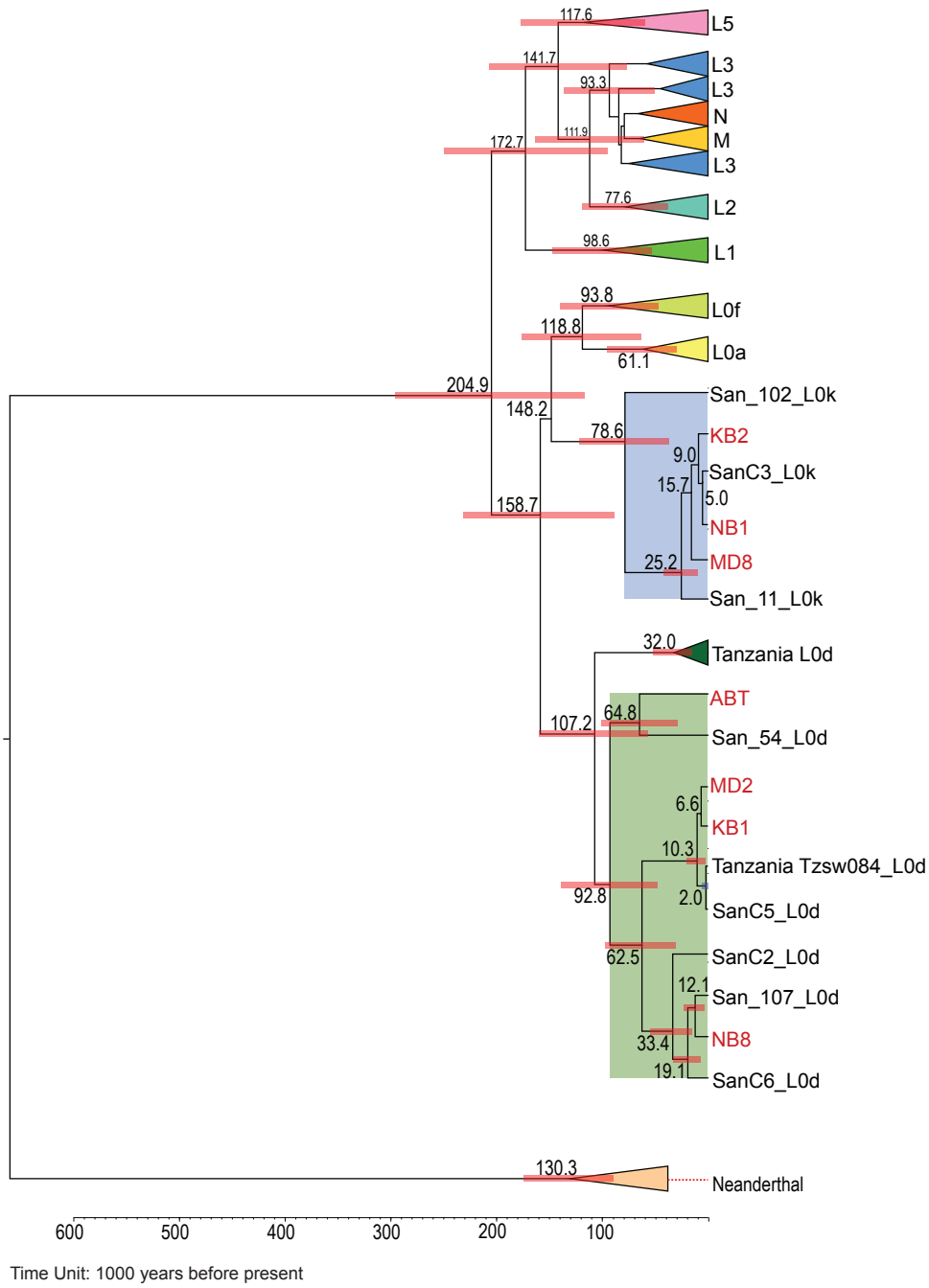

Supplementary Figure 1B. BEAST analysis of 158 individuals based on complete mitochondria. Individuals from this study are shown in red**.**

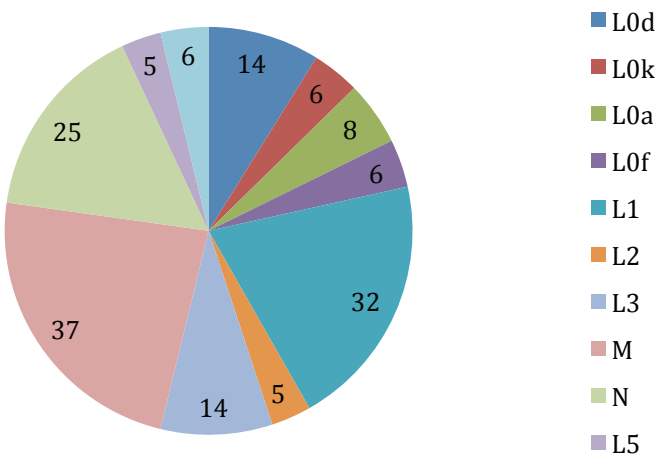

Supplementary Figure 1C. Haplogroup composition of the human mitochondrial samples used.

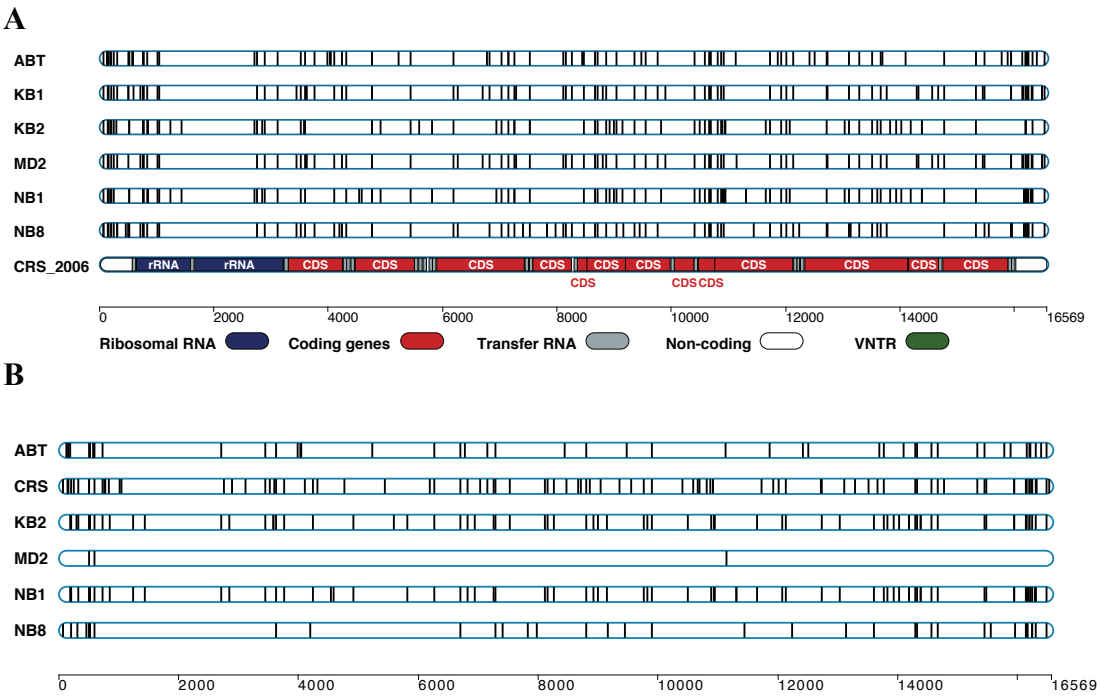

Supplementary Figure 2. Sequence differences in the southern African participants' mitochondrial genomes. A) using the Cambridge reference sequence (CRS) as a reference; B) Using KB1 as a reference.

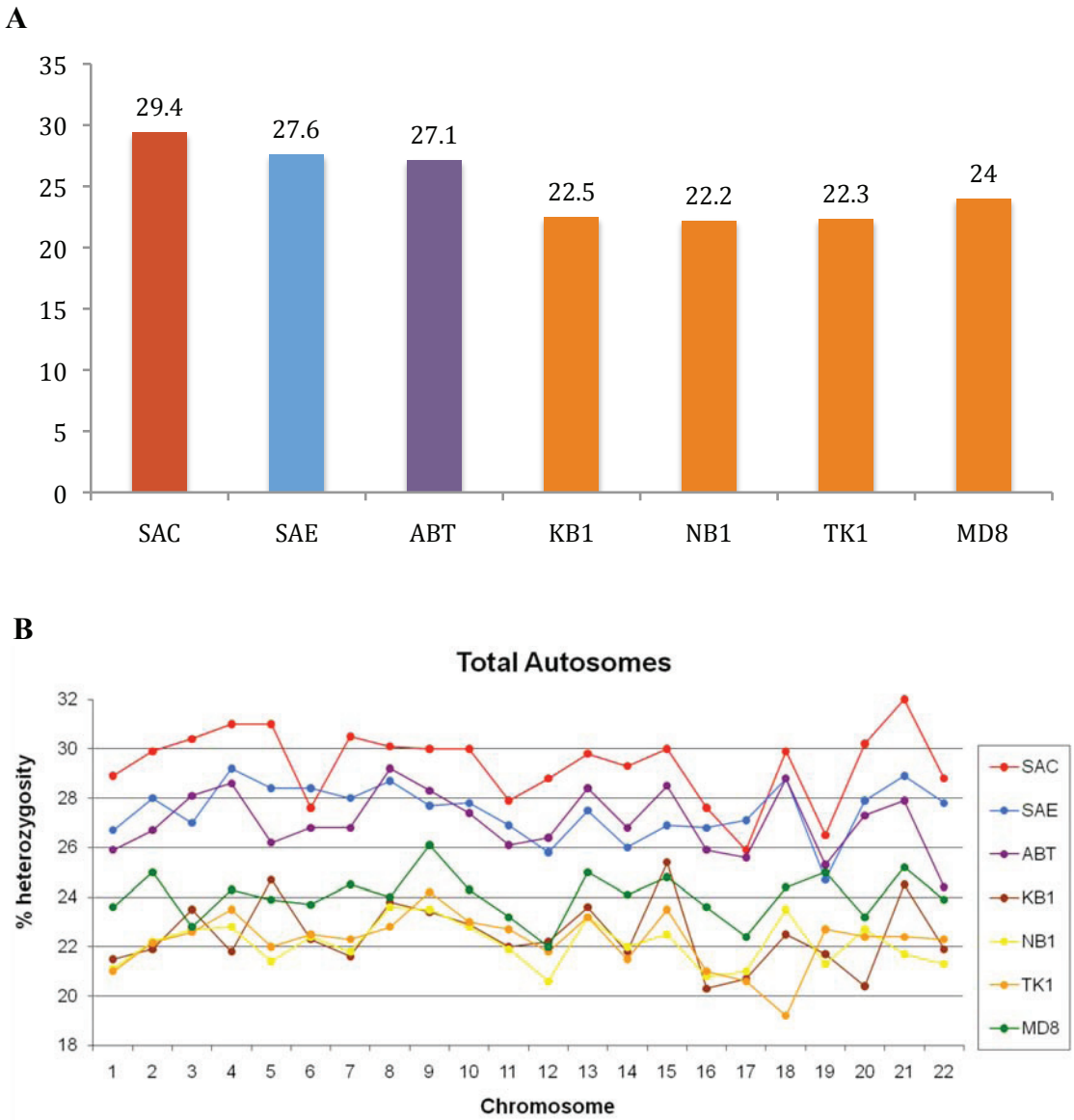

Supplementary Figure 3. Heterozygosity from genotyping data. Total (**A**) and per-autosome (**B**) genome-wide percentage heterozygosity for 1,105,569 autosomal SNPs in our five southern Africans compared to South African European (SAE) and admixed South African Coloured (SAC) samples. Total number of SNPs evaluated per chromosome: chr1, 95,287; chr2, 91,532; chr3, 75,838; chr4, 66,088; chr5, 68,079; chr6. 72,687; chr7. 60,929; chr8, 57,940; chr9, 49,319; chr10, 56,474; chr11, 56,274; chr12, 55,614; chr13, 39,234; chr14, 36,407; chr15, 33,933; chr16, 36,111; chr17, 34,644; chr18, 31,002; chr19, 27,235; chr20, 28,219; chr21, 14,906; and chr22, 17,817.

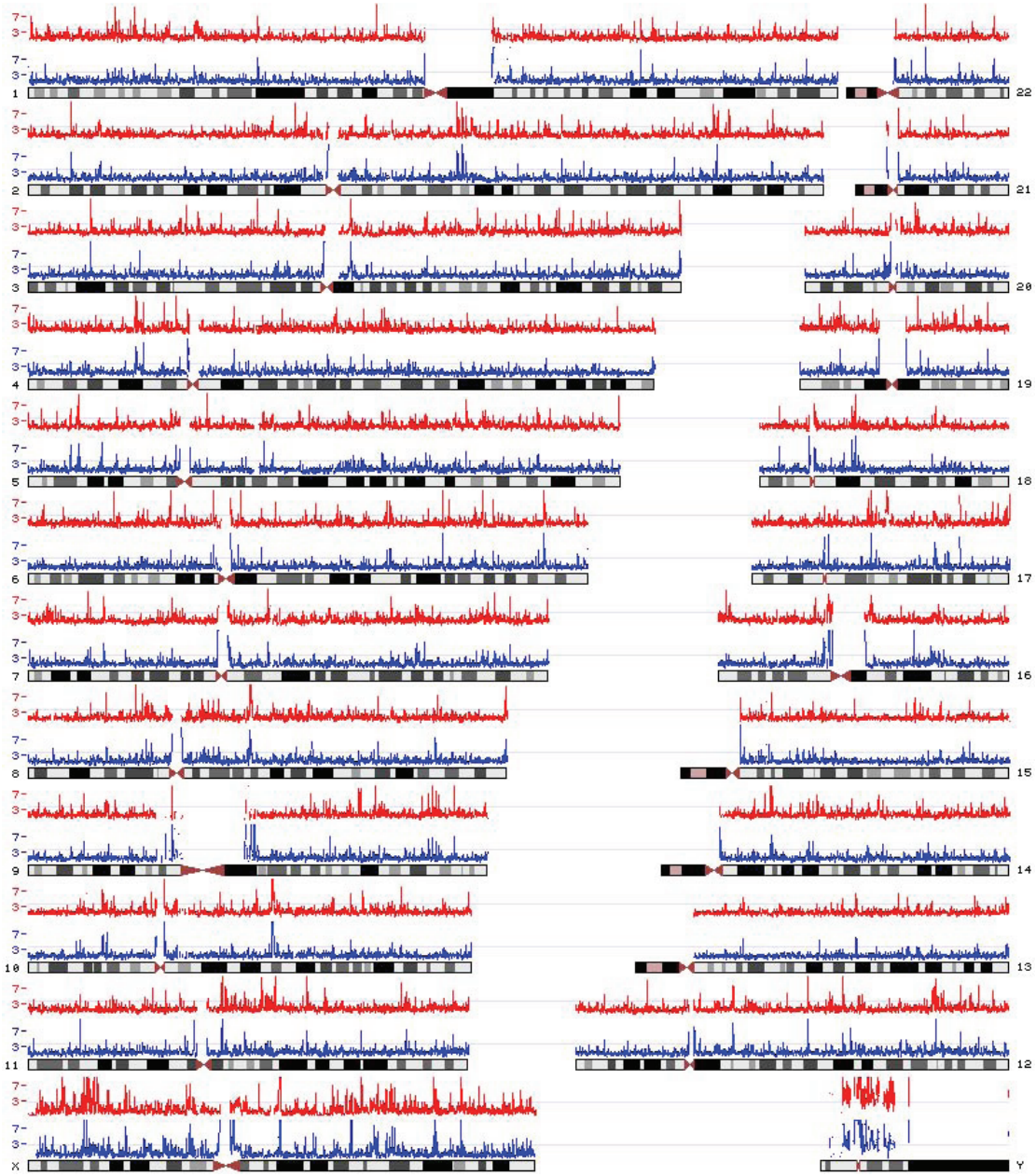

Supplementary Figure 4. Variation in SNP rate. Genome-wide SNP rates in KB1 (top, red) and ABT (bottom, blue), relative to the average for available human genomes.

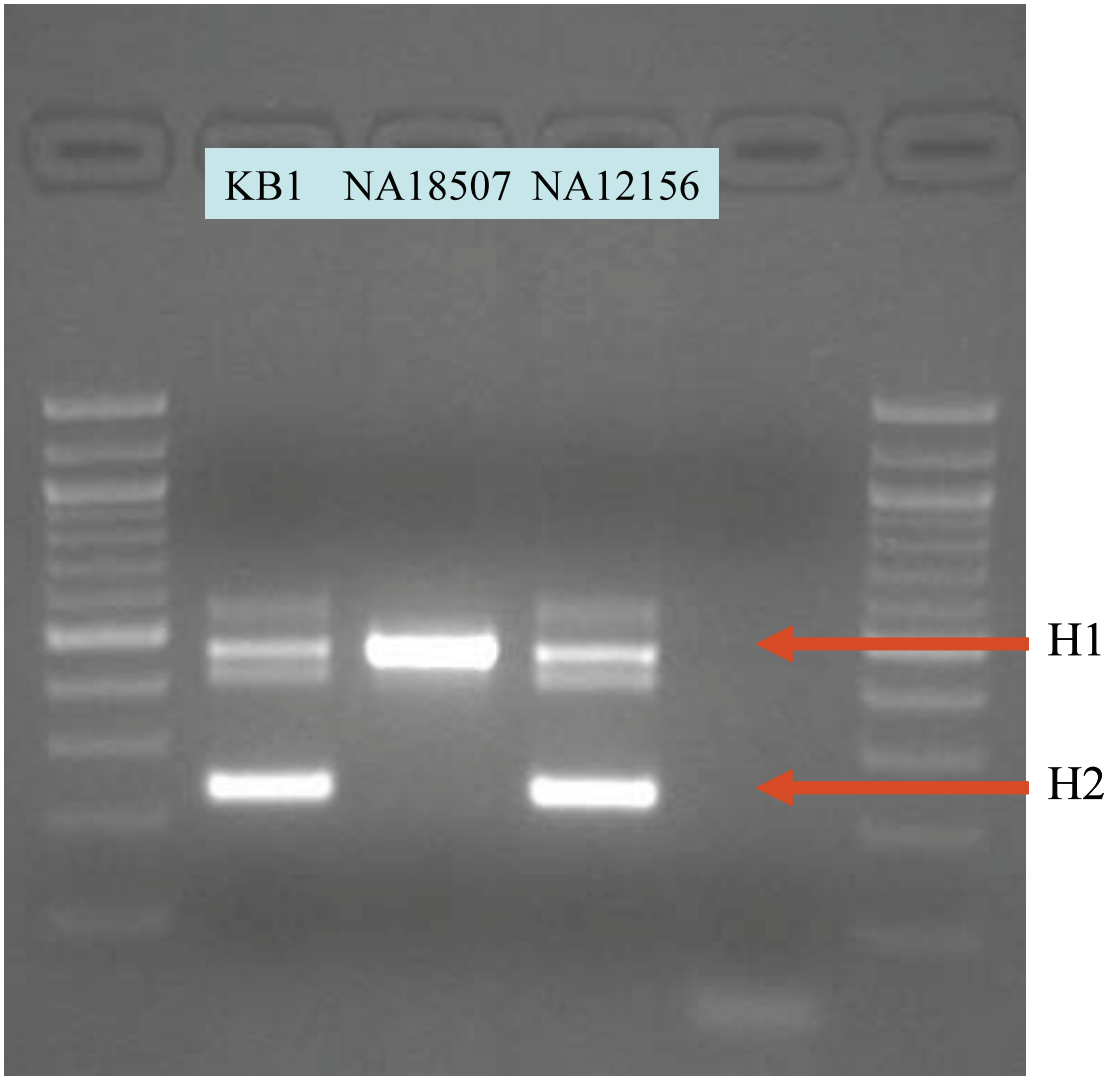

Supplementary Figure 5. Verification of the H2 inversion in KB1. Genotyping of a diagnostic indel confirms that KB1 is an H1/H2 heterozygote. Results for NA18507 (H1/H1) and NA12156 (H1/H2) are also shown. (See the main paper for a discussion.)

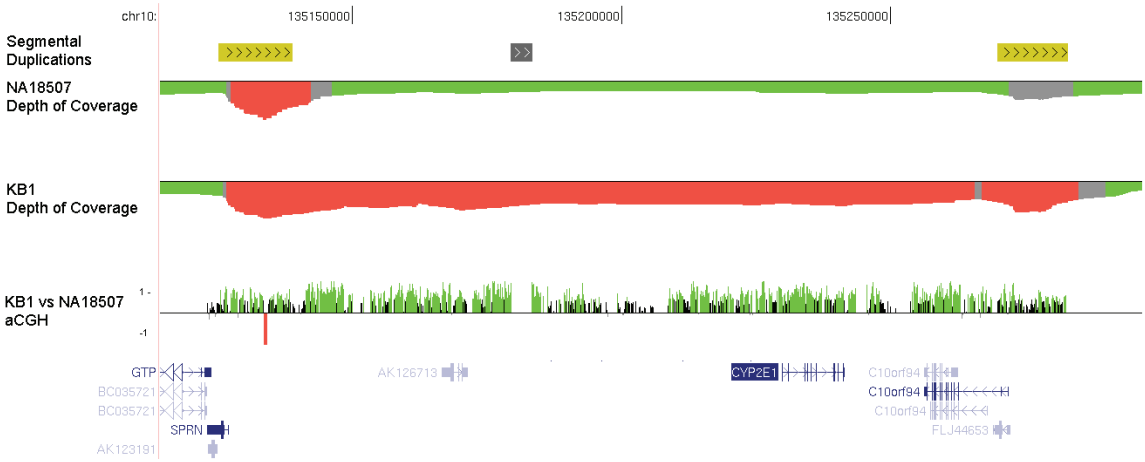

Supplementary Figure 6A. Validation of 140-kb duplication on chr10 in KB1. "aCGH" means array comparative genomic hybridization.

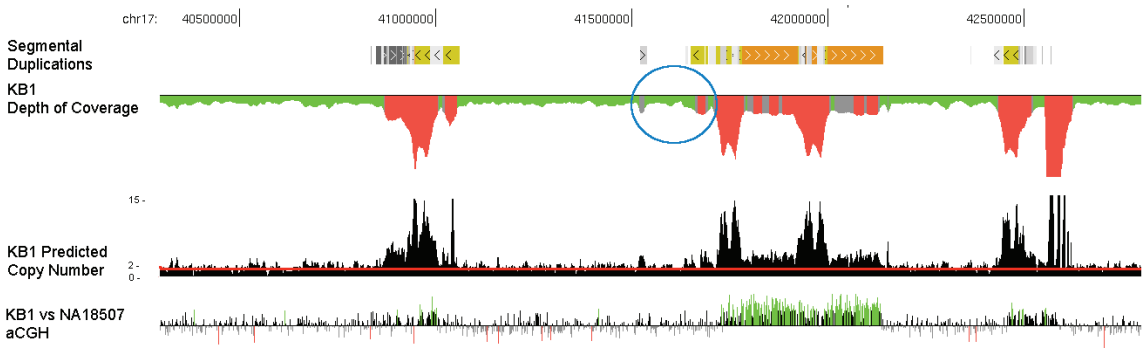

Supplementary Figure 6B. Estimated copy number for the 17q21.3 locus in KB1. The circled region corresponds to a segment found to be duplicated on all other examined H2 chromosomes. Read depth and array-CGH indicate that this duplication is not present in KB1.

Supplementary Figure 7. SNPs and interspecies alignments in the segment of the *LIPA* gene encoding the signal peptide. The first coding exon is shown, with translation into amino acids shown with blue background; the "minus" strand sequence is shown on the top line (reverse complement of the reference sequence's "plus" strand). Alignments (from the *multiZ* program) of the human sequence with those of many other placental mammals are shown, with red boxes around the alignment columns corresponding to the SNPs. SNPs from each of the genomes sequenced in this study are shown below the alignments as rectangles labeled by the nucleotide (homozygous) or nucleotides (heterozygous) ascertained in the indicated positions. Rectangle colors indicate that the frequency with which an allele was observed in the reads has been determined; this number and hyperlinks to the aligned reads can be obtained by clicking on the rectangle (in the live display of this figure). The last set of tracks shows the positions of SNPs for which phenotype-associated information can be obtained. The live display is available on the Penn State Genome Browser at http://main.genome-browser.bx.psu.edu/ .

A

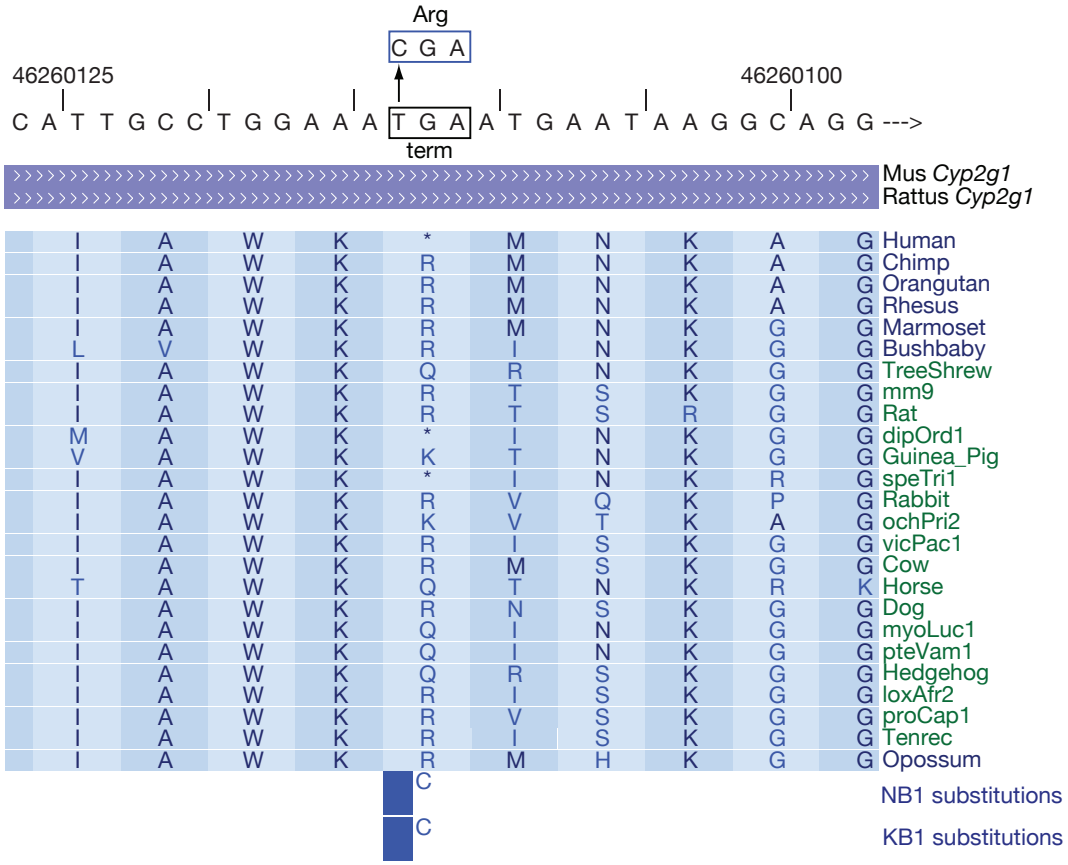

Supplementary Figure 8A. Retention of an active allele of *CYP2G* in Bushmen. A 30-base segment of the human reference genome assembly (hg18, March 2006, reverse complement of the standard sequence) from the gene *CYP2G* is given at the top of this diagram. It reads TGA at the center codon (a signal to stop translation of the mRNA), and thus this is not an active gene in most humans. However, both KB1 and NB1 are homozygous for the CGA codon (boxed in blue at the top, and shown in the variant tracks at the bottom), encoding an arginine and thus producing an active protein product similar to that shown for the mouse and rat *Cyp2g1* genes. Other primates and many other mammals also encode an arginine at this codon (multiple alignment in the middle), suggesting that this is the ancestral allele.

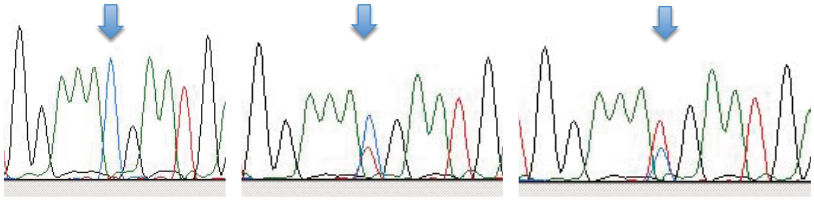

	CC	2C:1T	1C:2T	TT
White (n=11)	0	0	11	0
Bantu (n=29)	2	11	16	0
Bushmen (n=30)	8	11	11	0

Supplementary Figure 8B. Sanger-sequencing validation of the *CYP2G* SNP. Depicting homozygosity of the C-allele in KB1, and uneven allele distribution for MD8 (C:T = 2:1) and TK1 (C:T = 1:2). Further validation of 30 Bushmen, 29 Bantu, and 11 Europeans demonstrated a predominance of C-alleles in the Bushmen and T-alleles in Europeans.

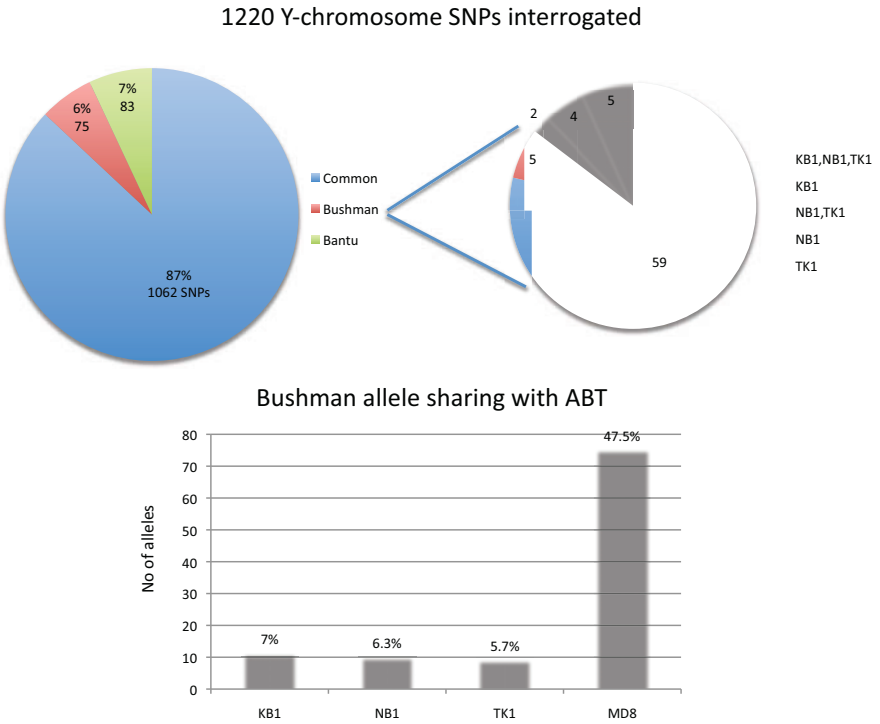

Supplementary Figure 9. Y-chromosome SNPs. Schematic overview of 1,220 Y chromosome SNPs genotyped on the Illumina 1M array for the five men, showing the number of shared alleles (1,062 SNPs), Bushmen-specific alleles (75 SNPs) and ABT-unique alleles (83 SNPs). Although 59 alleles are shared by KB1, NB1, and TK1, and a few others are unique to each of them, MD8 has no unique SNPs and shows the greatest Bantu-specific Y-allele sharing with ABT (common ancestral lineage E1b1).

Full Methods

Genome-wide genotyping

Whole-genome genotyping was performed using the Infinium HD technology with the current content of the Human 1M-Duo BeadChip, according to the standard protocol provided by the manufacturer (Illumina Inc., San Diego, CA, USA). The BeadChip was imaged with the Illumina BeadArray Reader (BeadStation 500G), and the Illumina BeadStudio software (version 3.2.32) was used for analysis of more than 1 million markers for the five selected individuals (KB1, NB1, TK1, MD8, and ABT), five additional Ju/'hoansi, and one additional Tuu, which were compared to those of a South African European (SAE) and South African Coloured (SAC). A GenCall score value of 0.5 was used as the cutoff to ensure the reliability of genotypes called.

Mitochondrial sequencing

Whole-genome shotgun libraries were constructed for samples from KB1, NB1, MD8, MD2, KB2, NB8, and ABT. Sufficient sequencing was performed to provide 16- to 134-fold coverage of each complete mitochondrial genome. Mitochondrial reads were identified by mapping to the Cambridge reference mitochondrial sequence, and were subsequently assembled by Newbler.

Exome sequencing

Large targeted regions can be enriched in a genomic sample using solid-phase programmable microarrays[44,45]. Although solution phase, hybridization selection, and enrichment have been performed using DNA and RNA probes followed by short-read sequencing (<100 bp), this combination of technologies yields low sequencing coverage for the middle of short targeted regions[46]. Currently, there are no reports of efficiently enriching the entire human exome.

Whole human exome sequencing was performed using a combination of Roche NimbleGen and Roche/454 sequencing technologies. An optimized, previously unpublished protocol was employed that efficiently used a total of 5 micrograms of genomic DNA. Previous studies have required 20 micrograms of starting material. A detailed description of the workflow is included below.

The Roche NimbleGen Whole Exome Array targets 175,278 exons covering 26,227,295 bp spanned by 197,218 probe regions covering 34,952,076 bp of the human genome. These exons represent approximately 16,000 protein-coding genes as defined in the Consensus Coding Sequencing (CCDS) project, build 36.2[35]. Chromosomal coordinates for the exon array design were obtained from the UCSC Genome Browser (human build hg18). Additionally, 551 human miRNA genes were targeted in the array and were identified using MiRBase (release 10). A total of 2.1 million probes were incorporated onto the array, targeting the forward strand and using a median probe length of 75 base pairs. Probe design has been previously described[44,45].

Sequence capture method

Protocol optimized for Roche 454 GS FLX Titanium:

5 µg of input genomic DNA is used to construct a sequencing library, following the protocol in sections 3.1 to 3.9 of the GS FLX *Titanium* General DNA Library Preparation Manual.

5 µg of input DNA is nebulized according to the Library Preparation Method Manual.

Nebulized DNA is purified using two columns from a MinElute PCR Purification kit (QIAGEN) according to the manufacturer's instructions.
Eluted DNA is size-selected using the Double SPRI selection method from the 454 General Library Preparation Method Manual.
Resulting DNA is analyzed using a BioAnalyzer DNA 7500 LabChip to ensure that the mean fragment size is between 500 and 800 bp and less than 10% of the library is below 350 bp or greater than 1,000 bp.
Material passing the above quality control is end-polished, has adaptors ligated, small fragments removed, and then a single-stranded DNA library is recovered using the methods from the Library Preparation Manual.

1 µL of the resulting sstDNA library is analyzed on a BioAnalyzer 6000 Pico chip and quality assessed based on Table 3-1 of the General Library Preparation Manual.

- The mean fragment size should be between 500 and 800 bp, and less than 10% of the DNA should be shorter than 350 bp or longer than 1,000 bp. The total yield of the library should be >3 ng, with the adaptor dimer peak less than 5% of the library peak height.

The samples are amplified using the Pre-Capture LM-PCR protocol in the NimbleGen *Titanium* Optimized Sequence Capture User Guide.

Amplified pre-capture LM-PCR material is purified using QIAquick (QIAGEN) columns and a modified protocol.

- 1,250 µL (5X) of Qiagen buffer PBI is added to each tube.
- The sample is applied to the QIAquick column and eluted in 50 µL of PCR-grade water.

The concentration and size distribution of the amplified library is determined using a BioAnalyzer DNA 7500 chip. Greater than 3 µg of DNA should be recovered from the pre-capture LM-PCR, with the same size characteristics given above.

Samples are hybridized and eluted according to the methods described in the NimbleGen *Titanium* Optimized Sequence Capture User Guide.

LM-PCR is done on captured samples according to the methods described in the NimbleGen *Titanium* Optimized Sequence Capture User Guide.

Post-capture LM-PCR material is cleaned up using the modified QIAquick column method indicated above.

1 µL of the post-capture LM-PCR is assessed using a BioAnalyzer DNA 7500 chip for the same criteria as above. A NanoDrop spectrophotometer is used to quantify the concentration and the A_{260}/A_{280} ratio.

qPCR is used to assess the enrichment success according to the methods described in the NimbleGen *Titanium* Optimized Sequence Capture User Guide.

The resulting library concentration is quantified by PicoGreen fluorometry.

Library emulsion PCR is then performed according to the GS FLX Titanium emPCR Preparation Manual, and the remaining workflow is identical to the standard GS FLX Titanium sequencing run.

Whole-genome sequencing of KB1

We employed previously described protocols[47,48], which were augmented as follows. Genomic DNA fragments extracted from blood samples of KB1 and NB1 were size-selected before DNA library construction by running the samples on a 2% unstained agarose gel along with a 100 bp DNA ladder (NE Biolabs). The ladder was excised and stained for fragment visualization, and for KB1 and NB1 we excised fragments between 400 and 1000 bp. The samples were then purified using the QIAquick Gel Extraction Kit from Qiagen and used for library construction according to the manufacturer's instructions (Roche Applied Sciences). These samples were sequenced on four Roche/454 GS FLX instruments using Titanium chemistry, for a total of 72 runs.

Computational methods

This section describes the details of the pipeline to call SNPs for KB1 and other Bushmen genomes from the sequence data produced by the Roche/454 GS-FLX sequencing instrument. The first step was to partition hg18 (the human reference genome used here) into intervals that would be uniquely mappable using reads of length 300 bp or more. The sequenced reads were then mapped to hg18 and assigned to one of the intervals. Newbler was then run on the reads in those intervals, and the SNPs were collected and transferred back to the original hg18 coordinates. After about 8X of the data was mapped, we examined the mapped intervals and discarded intervals that showed indications of pileup. These steps are described in greater detail below.

Single-coverage regions in hg18. The "single coverage" regions are intervals of hg18 that we expect sequenced human reads to map to uniquely. These were determined by aligning hg18 to itself with high stringency and finding the leftover intervals — those that did not align to some other part of hg18. Specific alignment details appear below, but we were looking for alignments of 300 bp or longer with at least 97% identity. Many identified repeats are uniquely mappable at this identity level. Further, some recent low copy number segmental duplications are not uniquely mappable at this level, even though they are not annotated as repeats in the human genome.

Approximately 49,000 single-coverage regions were identified. These are the regions between intervals that were parts of an hg18 self-alignment (also excluding regions with long runs of Ns). Lengths ranged from 1.7Mb down to a single base. Note that while short regions seem paradoxical — how can a one-base region be uniquely mappable? — in fact, this means that any 300-base read containing this position should be uniquely mappable.

Note that reads can occasionally map outside of single-coverage regions, as it's still possible for a read to uniquely map within a region where a strong self-alignment exists. This can happen in many ways, which are outside the scope of this document. Since our aim is to place reads into groups to be separately assembled, this is not a problem.

Self-alignment details. Lastz, a pairwise aligner that is freely available at

http://www.bx.psu.edu/miller_lab, was used to perform the self-alignment of hg18, with the goal of identifying all alignments with length ≥ 300 bases and identity ≥ 97%. This proved to be a challenge because of the presence of repeats (and repeats could not be excluded from this analysis). After some experimentation, we settled on a two-stage process using different scoring in each stage. Further, we were able to improve runtime by splitting the genome into 50-Mb chunks.

The first stage identified HSPs (high-scoring segment pairs, i.e., alignments without any gaps) using lastz with the following parameters, then post-processing to discard HSPs shorter than 100 bp. (Please see the lastz documentation for a more thorough explanation of these parameters.)

```
--step=32 --seed=match13 --notransitions --match=1,5 --hspthreshold=85
    --identity=97
```

Soft-masking (marking of repetitive sequences by lower-case letters) was removed from the input sequences so that repeat regions were included in the alignments. A step of 32 was chosen because our target alignment (300 bp, 97% identity) has at least 291 matches and no more than 9 mismatches. Assuming no indels, such an alignment has a probability of less than 1 in 1,000 of failing to contain a 44-base exact match. With
--step=32 and --seed=match13 we will find any exact match of length 44 or longer. With matches scoring 1 and mismatches –5, our target HSPs (97 matches and 3 mismatches) would score 82. However, the threshold of 85 also allows shorter, higher-identity HSPs. These were discarded using post-processing (before the second stage).

The second stage performs gapped alignment using the HSPs from the first stage. The following lastz parameters were used, with additional post-processing to discard alignments shorter than 300 bp.

```
--match=1,20 --gap=21,20 --ydrop=221 --gappedthreshold=102 --identity=97
```

Soft-masking was also removed in this stage. Here the mismatch scoring is much more stringent than for HSPs, and gap scoring is set to be nearly the same as for mismatches. Ydrop is set so that we will tolerate a run of about 10 mismatches. The target alignment (291 matches and 9 mismatches) would score 111 (the scoring threshold of 102 is thus a little lenient). Note that using these parameters in the first stage would have required an HSP threshold so low that the program would be overwhelmed by low-scoring HSPs.

The self-aligning intervals identified by this process were considered to be indistinguishable regions. They were combined by union, also including any run of 100 or more Ns in hg18. Intervals shorter than 500 bases were discarded, since these could possibly be bridged by a read aligning to the two flanking regions. The complement of the resulting set of intervals is the set of single-coverage intervals discussed in this report. There are 49,179 of these regions, with an average length of 54,821 bases. In total, they cover 2,696,041,061 bases, or 94.3% of the non-N portion of hg18.

Mapping KB1 reads

Seventy-seven sequencing runs from KB1 were compared to hg18. This was 83,331,226

trimmed reads comprising 29,165,432,509 bases (average length 350). The reads were aligned using lastz, and fall into four classes: mappable (84.5%), aligned but not uniquely mappable (5.4%), not alignable (9.7%), and uninformative (0.5%). (Uninformative reads are duplicates — only one of each group of duplicate reads is processed). The mapped reads comprised 26,100,525,922 bases, which represent 9.1X coverage of hg18 (excluding runs of Ns).

Alignment was performed using lastz with the following parameters:

```
--step=15 --seed=match13 --notransitions --exact=18 --maxwordcount=6 \
--match=1,3 --gap=1,3 --ydrop=10 --gappedthreshold=18 --identity=97 --coverage=90 \
--ambiguousn
```

Soft-masking was removed, allowing reads to align to repeats. A word-count limit of 6 corresponded to removing roughly 10% of the seed-word positions from last's internal table. Mapping was then performed by collecting any alignments for a given read. A read with only a single alignment, with identity ≥ 98%, was considered mappable. A read with more than one alignment, but with one having identity ≥ 98% and at least 1.5% better than the second best, was also considered mappable. There is a minor mistake here, in that any alignments with identity < 97% were discarded during the alignment stage. So it is possible that a read might have, say, one alignment at 98% and another at 96.6%, which should not pass the mappability criteria but which slips through as "mappable".

Calling KB1 SNPs from the whole-genome data

Each single-coverage interval was assigned a segment of the human reference sequence, consisting of the interval itself plus an additional 500 bp on each side to handle reads mapping at the ends of the single-coverage interval. The reads mapping to that segment were collected and the information about them extracted from the original SFF files. This included the complete untrimmed sequence, the quality values, and the flowgram information. This data was then combined to form an input SFF file, and supplied to Newbler as input. The SNP calls made by Newbler were then transferred to their original hg18 coordinates and then filtered to call SNPs only in the regions where we did not observe a pileup of reads.

Newbler details

This section describes the algorithm used by Newbler to call SNPs. The larger set of SNPs is called the AllDiffs set and it attempts to enumerate all the differences between the reference and the reads using less stringent filters and thresholds. For a SNP to be identified and reported, there must be at least two non-duplicate reads that (1) show the difference, (2) have at least 5 bases on both sides of the difference, and (3) have at most a few other isolated sequence differences in the read. In addition, if the –e option is used to set an expected depth, there must be at least 5% of that depth in differing reads. Finally, for single-base overcalls or undercalls to be reported, they must have a flow signal distribution that differs from that of the reads matching the reference (i.e., not all overcalls and undercalls are reported as SNPs). Once the SNP is identified, all reads that fully span the difference location and have at least 5 additional flanking nucleotides on both sides are used in reporting it.

Newbler designates a subset of these calls as High Confidence calls (HCDiffs). The general rules for this subset are:

1) There must be at least 3 non-duplicate reads containing the non-reference nucleotide, unless the –e option is specified, in which case at least 10% of the expected depth must contain it.
2) There must be both forward and reverse reads showing the difference, unless there are at least 5 reads with quality scores over 20 (or 30 if the difference involves a 5-mer or higher).
3) If the difference is a single-base overcall or undercall, the reads with the non-reference nucleotide must form the consensus of the sequenced reads (i.e., at that location, the overall consensus must differ from the reference) and the signal distribution of the differing reads must vary from the matching reads (and the number of bases in that homopolymer of the reference).

Heterozygous vs. homozygous
SNP calls for KB1, NB1, MD8, TK1, and ABT were made from 454 data. We use a simple metric, AAF (alternate allele frequency), to call a SNP heterozygous vs. homozygous. For all of these samples, the SNP was called homozygous if the alternate allele frequency was greater than or equal to 80%.

Adding exome-capture sequences to the whole-genome data for KB1
We compared the SNP calls from the whole-genome fragment (non-paired-end) sequences to those from the exome-captured sequences, in order to validate the sequences and their subsequent analyses. For KB1, we called 3,536,132 SNPs using 9.13X whole-genome fragment sequences, and 122,392 SNPs using 16-fold exome sequences. 99,372 of the locations were common between the two sets of SNP calls. The difference was largely related to the heterozygosity of the location. We found that in some cases one set included a homozygous call, whereas the other set included a heterozygous call, and this was usually due to read coverage at the location.

Using Illumina to validate the KB1 SNP calls
We used 23.2-fold mapped Illumina whole-genome data to verify the 454 SNP calls. We used MAQ with default parameters to call a liberal set of SNPs from the data. We also called a high-confidence subset using single-end mapping quality scores and discarding abnormal pairs. We required that a read have a minimum mapping quality of 10, the SNP location have a read depth between 6 and 75, and the SNPs not be within 10 bp of an indel. Furthermore, we filtered to keep only SNPs in regions that we deemed mappable using the 454 reads. We called 4,215,263 liberal and 3,835,844 high-confidence SNPs from the Illumina data. 2,943,320 of the 3,594,898 SNP calls made using 454 sequences were confirmed using those made from the Illumina sequences. Further analysis showed that lack of coverage was the major reason for the discrepancies between the calls from the two technologies. This was also the primary reason that we decided to pool the 454 and Illumina SNP calls to create a single final set of SNPs for KB1.

Using genotyping data to validate the KB1 SNP calls
We used the forward strand output from BeadStudio and the actual strand of the alleles from dbSNP to infer the genotypes on the genome-wide array. We filtered the genotype information to remove indels, and sorted it into two separate sets: one for locations with reference sequence matches and the other for the SNP calls. Then, we computed two separate intersections, using

only the positions of the sequence SNPs intersecting the genotype SNPs and the sequence SNPs intersecting the reference sequence matches. We computed the false-negative rate (0.09) by taking the number of genotype SNP calls that were missed (not called) by the sequencing and dividing this by the total number of genotype SNPs. The false-positive rate (0.0009) was calculated by taking the number of sequence SNPs intersecting the reference sequence matches divided by the number of reference sequence matches.

The final set of KB1 SNP calls

The following rules were used to pool the SNP calls to form the final set of KB1 SNPs.

1) All SNPs from the genotyping array were included.
2) A high-confidence SNP call from 454 sequence data was *not* included in the final set, if any of the following was found to be true:
    1. If the 454 call was a homozygous SNP and there was no evidence supporting the variant allele in the uniquely mapped Illumina reads. This rule was only applied to regions with more than 3 uniquely mapped Illumina reads.
    2. If the 454 call wass a heterozygous SNP and there was no evidence supporting the variant allele in the uniquely mapped Illumina reads. Only regions with an Illumina coverage of 10 or greater were considered for this rule.
3) A high-confidence SNP call using the Illumina data was *not* included in the final set, if any of the following was found to be true:
    1. If the Illumina call was a homozygous SNP, coverage by 454 reads at that location was greater than 3, and it was not called a SNP using 454 data.
    2. If the Illumina call was a heterozygous SNP, coverage by 454 reads at that location was 10 or greater, and it was not called a SNP using 454 data.
4) A SNP was included if it was called in the liberal SNP set using both 454 and Illumina sequences.
5) All SNPs at locations with more than two alleles were discarded.

These rules were used to decide the locations that would be included in the final set of SNPs. The genotype calls for the final set were made using the following rules:

1) If the location was present on the genome-wide array, the genotype call from the array was selected.
2) If the location was not present on the genome-wide array, the genotype call for the technology with the higher coverage was selected. If the number of reads from 454 exceeded the number of reads from Illumina at that location, the 454 call was accepted as the consensus, and vice-versa.

Whole-genome SOLiD sequencing of ABT

The genome of ABT was sequenced to over 30-fold coverage using Applied Biosystems' short-read technology, SOLiD, including 50-base paired-ends of various insert lengths (2,713,797,283 50-base fragments; 120,825,147 25-base paired reads; 567,425,404 50-base paired reads). Genomic libraries were constructed from blood-extracted DNA with an average insert size of 3-5

kb. A total of 4,379,849 SNPs were called using the SOLiD System Software for primary and secondary analysis. Further filtering reduced the number of SNP calls to 3,624,334.

Whole-genome Illumina sequencing of ABT

We used 7.2-fold mapped Illumina data to verify the SOLiD SNP calls. Mapping and SNP calling were performed as described above. We called 2,894,707 liberal and 2,040,551 high-confidence SNPs from the Illumina data. 2,366,494 of the 3,624,334 SNP calls made using SOLiD sequences were confirmed using those made from the Illumina sequences. As with KB1, lack of coverage was the major reason for the discrepancies between the calls from the two technologies.

Large-insert paired-end sequencing of KB1

Sixteen runs on the Roche/454 GS FLX platform were performed on large-insert paired-end libraries. A total of 18.8 million reads and 6.4Gb were sequenced. 3.4% of the reads were discarded as uninformative (i.e., an exact duplicate of another read; only one read per group of duplicates was kept for coverage calculations). The number of duplicate reads varied from less than 1% to 15% per run.

About one quarter (26.4%) of the reads did not have the linker present that separates the two ends. In 12.2% of all cases the linker region was too close to one end (less than 18 bp) or had a double linker (the latter in only about 0.1%). The remaining 61.3% were used for assembling the data, computing clone coverage, and detecting copy-number variations. Our in-house mapping algorithm (lastz) was able to map 37% more of he reads to the human reference assembly than the Newbler software from the manufacturer.

An additional 5% of the reads were then filtered out due to their extreme predicted insert size, either too short or too long (the shortest and longest 2.5% of the insert lengths). In total, 43.5% of the paired ends were successfully mapped and kept. The average insert length was determined to be 10.6 kb. The inserts covered 86.6 Gb (clone coverage), which is 30.9 times the number of bases sequenced (mappable genome size is 2.8 Gb). Insert sizes from a total of 19 different libraries were consistent with the following three distinct profiles: Eight runs had insert size distribution of 12 kb average, 8 kb min, 18 kb max. Six runs had had 10 Kb average with 7K min and 15K max insert size, while wo other runs had a 7 kb average with 5kb min and 13kb max.

Personal genomes used in this study but sequenced elsewhere

Genome	Sequence Method; Project	
Craig Venter (JCVI)[49]	Sanger	Dr. Venter's single-base variants from the file HuRef.InternalHuRef-NCBI.gff, filtered to include only "method 1" variants (i.e., where the variant was kept in its original form and not post-processed), and to exclude any variants that had N as an allele. The J. Craig Venter Institute hosts a genome browser.
James Watson (CSHL)[13]	Roche/454 (FLX)	These single-base variants came from the file watson_snp.gff.gz. Cold Spring Harbor Lab hosts a genome browser.
Yoruba NA18507[41]	Illumina/Solexa	Illumina released the read sequences to the NCBI Short Read Archive. Aakrosh Ratan (see author list) mapped the sequence reads to the human reference assembly and called single-base variants using MAQ.
YH (Han Chinese)[50]	YanHuang Project	The YanHuang Project released these single-base variants from the genome of a Han Chinese individual. The data are available from the YH database in the file yhsnp_add.gff. The YanHuang Project hosts a genome browser.
SJK (Seong-Jin Kim; Korean)[51]	Illumina	Researchers at Gachon University of Medicine and Science (GUMS) and the Korean Bioinformation Center (KOBIC) released these single-base variants from the genome of Seong-Jin Kim. The data are available from KOBIC in the file KOREF-solexa-snp-X30_Q40d4D100.gff.
NA12891 (CEU Trio Father), NA12892 (CEU Trio Mother), NA19240 (Yoruba YRI Trio Daughter)	The 1000 Genomes Project (unpublished)	

Novel SNPs

A SNP is normally labeled "novel" if it has not previously been published. To determine which SNPs were novel in the genomes sequenced elsewhere, we had to account for the subsequent addition of those SNPs to collective databases. Therefore we used dbSNP version 126, which pre-dates the personal genomes, instead of a more recent dbSNP release. We then treated all of the personal genomes sequenced elsewhere as if each had been published after the others. Thus, in this study, "novel" means that the SNP is not in dbSNP126, any of the other personal genomes listed in the table above, PhenCode[52], the Environmental Genome Project[53], or ENCODE[54] resequencing. In the case of indels, any overlap with a polymorphic site called in the other data sources led to its characterization as *not* being novel. For instance, a 10-bp deletion not seen in any other genome but overlapping a single nucleotide change in some individual makes does not qualify as novel. Similarly, for substitutions a new allele at a previously-known SNP location does not count as novel either.

Figure 3A and the chromosome 17 hotspot

For the genome-wide SNP rates in the KB1 and ABT genomes, SNPs in each (tiled) 50-kb window were counted, including those from six genomes obtained from other sources. The counts for KB1 and ABT were divided by the average count for the other six to obtain a ratio of over-enrichment for each window. Those ratios are plotted in Supplementary Figure 4.

For Figure 3A in the main paper we proceeded as follows. In non-overlapping 50-kb windows across the autosomes, we determined the average number of KB1 SNPs per kilobase of single-copy sequence (see above). We noted an unusually high frequency of SNPs in a 15-window (750-kb) interval of chromosome 17, at positions 41,000,000-41,750,000 in the coordinates of NCBI Build 36. Although nearby regions on both flanks contain near-identical segmental duplications, the interval itself is essentially free of such duplications in both Build 36

and KB1.

To measure the statistical significance of this hotspot, we performed the following randomization experiment. We ranked the autosomal windows by decreasing SNP rate, discarding windows having less than 10 kb of single-copy sequence. A collection of windows with the same SNP rate were re-ranked so that each was given the average of their original ranks. Of the 52,341 remaining windows, those in the putative hotspot had ranks 410, 9780, 178, 347, 7740, 151, 164, 230, 398, 792, 631, 702, 1007, 3378, and 152, whose sum is 26,060. Starting with the list of ranks (after re-ranking to handle identical SNP rates), we performed 100,000 randomizations of the list (using the so-called Fisher-Yates shuffle), and, in each case, determined whether any 15 consecutive numbers (of the 52,341 shuffled ranks) had a sum of 26,060 or less. That condition was never met in the 100,000 simulated events, giving an empirical *p*-value of less than 10^{-5}.

To enable direct comparison of SNP rates from several genomes, we computed the autosome-wide average number of SNPs per single-copy kilobase for each genome. That is, we computed the total number of SNPs in single-copy regions (of NCBI Build 36) and divided by the number of single-copy kilobases (2,584,574). The resulting numbers are as follows:

KB1	0.9256
NB1	0.1312
ABT	1.3043
NA18507	0.9892
NA19240	1.3329
Watson	0.7706
Venter	1.1208
YH (Chinese)	1.1519
SJK (Korean)	1.2841

In the region of chromosome 17 pictured in Fig. 3A, we determined SNPs per single-copy kilobase, then divided by that genome's autosome-wide average.

Predicting which amino-acid changes may have functional consequences

Amino-acid changes are more likely to be deleterious if they occur in a functional site and [55]substitute an amino acid with different biochemical properties from the original. Several computational tools use this principle to predict which protein polymorphisms are likely to be detrimental. Another useful computational resource is MODBASE[56], a database providing information about protein structure models, which help in predicting the structurally and functionally important sites of a protein sequence. Here, we describe a pipeline that we use to identify putative deleterious SNPs.

First, we use an in-house program named ModelFinder to identify putative functional SNPs by using protein structure model information (also used in ref 48). Our assumption is that SNPs within a modeled sequence have a higher likelihood of being deleterious, because the 3D structure provides the protein with a particular functionality. ModelFinder uses amino-acid sequence and SNP information as the input, locating the protein information for each SNP by using the UCSC annotation database[57], and querying MODBASE to determine if the residue is covered by a model structure. The model score and sequence identity with the model template for the covered SNPs are also obtained. In addition, the phastCons[58] score and Blosum62[59] score are obtained for these SNP sites, to measure the conservation level among 44 species and various protein families. The residues with high conservation levels are expected to be more important functionally. Subsequently, another program attempts to map these potentially deleterious SNPs

to known disease-associated genes in the OMIM database. We combine these sources of information to predict which observed amino-acid-changing SNPs are likely to have a functional consequence. The following table indicates how many of the amino-acid-changing SNPs in each of our five participants scored using these criteria.

	# of novel SNPs	# of putative functional SNPs		# of putative functional SNPs with phastCons>0.8		# of putative functional SNPs involved in OMIM genes	
		#	% in novel SNPs	#	% in putative SNPs	#	% in putative SNPs
ABT	2923	851	29.11%	664	78.03%	519	60.99%
MD8	2559	705	27.55%	503	71.38%	456	64.68%
KB1	3592	912	25.39%	660	72.37%	565	61.95%
NB1	3096	828	26.74%	560	67.63%	502	60.63%
TK1	3116	865	27.76%	660	76.3%	546	63.12%

Validating predicted duplications

Genomic DNA fragments from KB1 and NA18507 were labeled and hybridized against a NimbleGen genome-wide tiling microarray (2.1 million HD2). We also designed a custom array (12-plex, 135,000) targeted toward regions of predicted copy-number difference. On the targeted array, the probe intensities from a pair of reverse-labeling experiments were averaged together. Targeted analysis was performed for each predicted interval greater than 20 kb. The mean log2 intensities for each interval were compared with the signals from a set of control regions using a single-tailed unequal-variance t-test. Validation status was determined using a false discovery rate threshold of 0.01[60].

Supplementary References

1 Westphal, E. O. J., in *Current trends in linguistics* (Mouton, The Hague, 1971), Vol. 7, pp. 367.

2 Smith, A., Malherbe, C., Guenther, M. & Berens, P., *The Bushmen of Southern Africa: a foraging society in transition.* (David Philip Publishers, Cape Town, 2004).

3 Oota, H. et al., Human mtDNA and Y-chromosome variation is correlated with matrilocal versus patrilocal residence. *Nat Genet* **29** (1), 20 (2001).

4 Karafet, T. M. et al., New binary polymorphisms reshape and increase resolution of the human Y chromosomal haplogroup tree. *Genome Res* **18** (5), 830 (2008).

5 Cruciani, F. et al., A back migration from Asia to sub-Saharan Africa is supported by high-resolution analysis of human Y-chromosome haplotypes. *Am J Hum Genet* **70** (5), 1197 (2002).

6 Working Group of Indigenous Minorities in Southern Africa, WIMSA, Available at http://www.wimsanet.org/news, (2009).

7 Patterson, N. et al., Genetic structure of a unique admixed population: implications for medical research. *Hum Mol Genet* (2009).

8 Berniell-Lee, G. et al., Admixture and sexual bias in the population settlement of La Reunion Island (Indian Ocean). *Am J Phys Anthropol* **136** (1), 100 (2008).

9 Coelho, M. et al., On the edge of Bantu expansions: mtDNA, Y chromosome and lactase persistence genetic variation in southwestern Angola. *BMC Evol Biol* **9**, 80 (2009).

10 Pilkington, M. M. et al., Contrasting signatures of population growth for mitochondrial DNA and Y chromosomes among human populations in Africa. *Mol Biol Evol* **25** (3), 517 (2008).

11 Pearson, C. E., Nichol Edamura, K., and Cleary, J. D., Repeat instability: mechanisms of dynamic mutations. *Nat Rev Genet* **6** (10), 729 (2005).

12 Garber, M. et al., Closing gaps in the human genome using sequencing by synthesis. *Genome Biol* **10** (6), R60 (2009).

13 Wheeler, D. A. et al., The complete genome of an individual by massively parallel DNA sequencing. *Nature* **452** (7189), 872 (2008).

14 Ingram, C. J. et al., Lactose digestion and the evolutionary genetics of lactase persistence. *Hum Genet* **124** (6), 579 (2009).

15 Han, J. et al., A genome-wide association study identifies novel alleles associated with hair color and skin pigmentation. *PLoS Genet* **4** (5), e1000074 (2008).

16 Nalls, M. A. et al., Admixture mapping of white cell count: genetic locus responsible for lower white blood cell count in the Health ABC and Jackson Heart studies. *Am J Hum Genet* **82** (1), 81 (2008).

17 Reich, D. et al., Reduced neutrophil count in people of African descent is due to a regulatory variant in the Duffy antigen receptor for chemokines gene. *PLoS Genet* **5** (1), e1000360 (2009).

18 Miller, L. H., Mason, S. J., Clyde, D. F., and McGinniss, M. H., The resistance factor to Plasmodium vivax in blacks. The Duffy-blood-group genotype, FyFy. *N Engl J Med* **295** (6), 302 (1976).

19 He, W. et al., Duffy antigen receptor for chemokines mediates trans-infection of HIV-1 from red blood cells to target cells and affects HIV-AIDS susceptibility. *Cell Host Microbe* **4** (1), 52 (2008).

20 Langhi, D. M., Jr. and Bordin, J. O., Duffy blood group and malaria. *Hematology* **11** (5), 389 (2006).

21 Escalante, A. A. et al., A monkey's tale: the origin of Plasmodium vivax as a human malaria parasite. *Proc Natl Acad Sci U S A* **102** (6), 1980 (2005).

22 Sheng, J. et al., Characterization of human CYP2G genes: widespread loss-of-function mutations and genetic polymorphism. *Pharmacogenetics* **10** (8), 667 (2000).

23 Itsara, A. et al., Population analysis of large copy number variants and hotspots of human genetic disease. *Am J Hum Genet* **84** (2), 148 (2009).

24 Hoeg, J. M., Demosky, S. J., Jr., Pescovitz, O. H., and Brewer, H. B., Jr., Cholesteryl ester storage disease and Wolman disease: phenotypic variants of lysosomal acid cholesteryl ester hydrolase deficiency. *Am J Hum Genet* **36** (6), 1190 (1984).

25 Zschenker, O. et al., Characterization of lysosomal acid lipase mutations in the signal peptide and mature polypeptide region causing Wolman disease. *J Lipid Res* **42** (7), 1033 (2001).

26 Wiebusch, H. et al., A novel missense mutation (Gly2Arg) in the human lysosomal acid lipase gene is found in individuals with and without cholesterol ester storage disease (CESD). *Clin Genet* **50** (2), 106 (1996).

27 Lalueza-Fox, C. et al., Bitter taste perception in Neanderthals through the analysis of the TAS2R38 gene. *Biol Lett* (2009).

28 Wooding, S. et al., Independent evolution of bitter-taste sensitivity in humans and chimpanzees. *Nature* **440** (7086), 930 (2006).

29 Dickson, R. C., The normal hearing of Bantu and Bushmen. A pilot study. *J Laryngol Otol* **82** (6), 505 (1968).

30 Jarvis, J. F. and Van Heerden, H. G., The acuity of hearing in the Kalahari Bushmen . A pilot survey. *J Laryngol Otol* **81** (1), 63 (1967).

31 Bork, J. M. et al., Usher syndrome 1D and nonsyndromic autosomal recessive deafness DFNB12 are caused by allelic mutations of the novel cadherin-like gene CDH23. *Am J Hum Genet* **68** (1), 26 (2001).

32 Eudy, J. D. et al., Mutation of a gene encoding a protein with extracellular matrix motifs in Usher syndrome type IIa. *Science* **280** (5370), 1753 (1998).

33 Wood, E. T. et al., Contrasting patterns of Y chromosome and mtDNA variation in Africa: evidence for sex-biased demographic processes. *Eur J Hum Genet* **13** (7), 867 (2005).

34 International Society of Genealogy Y-DNA Haplogroup Tree, Available at http://www.isogg.org/tree/index09.html, (2009).

35 Pruitt, K. D. et al., The consensus coding sequence (CCDS) project: Identifying a common protein-coding gene set for the human and mouse genomes. *Genome Res* **19** (7), 1316 (2009).

36 McDougall, I., Brown, F. H., and Fleagle, J. G., Stratigraphic placement and age of modern humans from Kibish, Ethiopia. *Nature* **433** (7027), 733 (2005).

37 Noonan, J. P. et al., Sequencing and analysis of Neanderthal genomic DNA. *Science* **314** (5802), 1113 (2006).

38 Gonder, M. K. et al., Whole-mtDNA genome sequence analysis of ancient African lineages. *Mol Biol Evol* **24** (3), 757 (2007).

39 Green, R. E. et al., A complete Neandertal mitochondrial genome sequence determined by high-throughput sequencing. *Cell* **134** (3), 416 (2008).

40 Briggs, A. W. et al., Targeted retrieval and analysis of five Neandertal mtDNA genomes. *Science* **325** (5938), 318 (2009).

41 Bentley, D. R. et al., Accurate whole human genome sequencing using reversible terminator chemistry. *Nature* **456** (7218), 53 (2008).

42 Salas, A. et al., The making of the African mtDNA landscape. *Am J Hum Genet* **71** (5), 1082 (2002).

43 Caswell, J. L. et al., Analysis of chimpanzee history based on genome sequence alignments. *PLoS Genet* **4** (4), e1000057 (2008).

44 Albert, T. J. et al., Direct selection of human genomic loci by microarray hybridization. *Nat Methods* **4** (11), 903 (2007).

45 Okou, D. T. et al., Microarray-based genomic selection for high-throughput resequencing. *Nat Methods* **4** (11), 907 (2007).

46 Herman, D. S. et al., Filter-based hybridization capture of subgenomes enables resequencing and copy-number detection. *Nat Methods* **6** (7), 507 (2009).

47 Margulies, M. et al., Genome sequencing in microfabricated high-density picolitre reactors. *Nature* **437** (7057), 376 (2005).

48 Miller, W. et al., Sequencing the nuclear genome of the extinct woolly mammoth. *Nature* **456** (7220), 387 (2008).

49 Levy, S. et al., The diploid genome sequence of an individual human. *PLoS Biol* **5** (10), e254 (2007).

50 Wang, J. et al., The diploid genome sequence of an Asian individual. *Nature* **456** (7218), 60 (2008).

51 Ahn, S. M. et al., The first Korean genome sequence and analysis: full genome sequencing for a socio-ethnic group. *Genome Res* **19** (9), 1622 (2009).

52 Giardine, B. et al., PhenCode: connecting ENCODE data with mutations and phenotype. *Hum Mutat* **28** (6), 554 (2007).

53 National Institute of Environmental Health Sciences' Environmental Genome Project, Available at http://egp.gs.washington.edu, (2009).

54 International HapMap Project: ENCODE Data, Available at http://www.hapmap.org/downloads/encode1.html.en#Reseq, (2009).

55 Sunyaev, S., Ramensky, V., and Bork, P., Towards a structural basis of human non-synonymous single nucleotide polymorphisms. *Trends Genet* **16** (5), 198 (2000).

56 Pieper, U. et al., MODBASE: a database of annotated comparative protein structure models and associated resources. *Nucleic Acids Res* **34** (Database issue), D291 (2006).

57 Kuhn, R. M. et al., The UCSC genome browser database: update 2007. *Nucleic Acids Res* **35** (Database issue), D668 (2007).

58 Siepel, A. et al., Evolutionarily conserved elements in vertebrate, insect, worm, and yeast genomes. *Genome Res* **15** (8), 1034 (2005).

59 Henikoff, S. and Henikoff, J. G., Amino acid substitution matrices from protein blocks. *Proc Natl Acad Sci U S A* **89** (22), 10915 (1992).

60 Storey, J. D. and Tibshirani, R., Statistical significance for genomewide studies. *Proc Natl Acad Sci U S A* **100** (16), 9440 (2003).